Astron. Astrophys. 267, 410–432 (1993)

ASTRONOMY
AND
ASTROPHYSICS

# Synthetic AGB evolution

## I. A new model

**M.A.T. Groenewegen**[1] **and T. de Jong**[1,2]

[1] Astronomical Institute "Anton Pannekoek", Kruislaan 403, NL-1098 SJ Amsterdam, The Netherlands
[2] SRON, Space Research Groningen, P.O. Box 800, NL-9700 AV Groningen, The Netherlands

Received May 4, accepted July 6, 1992

**Abstract.** We have constructed a model to calculate in a synthetic way the evolution of stars on the asymptotic giant branch (AGB). The evolution is started at the first thermal pulse (TP) and is terminated when the envelope mass has been lost due to mass loss or when the core mass reaches the Chandrasekhar mass.

Our model is more realistic than previous synthetic evolution models in that more physics has been included. The variation of the luminosity during the interpulse period is taken into account as well as the fact that, initially, the first few pulses are not yet at full amplitude and that the luminosity is lower than given by the standard core–mass–luminosity relations. Most of the relations used are metallicity dependent to be able to make a realistic comparison with stars of different metallicity. The effects of first, second and third dredge-up are taken into account. The effect of hot bottom burning (HBB) is included in an approximate way. Mass loss on the AGB is included through a Reimers Law. We also included mass loss prior to the AGB.

The free parameters in our calculations are the minimum core mass for dredge-up ($M_c^{\rm min}$), the third dredge-up efficiency ($\lambda$) and three mass loss scaling parameters ($\eta_{\rm RGB}$, $\eta_{\rm EAGB}$, $\eta_{\rm AGB}$).

The model has been applied to the LMC using a recent determination of the age–metallicity and star formation rate (SFR) for the LMC. The observed carbon star luminosity function and the observed ratio of oxygen-rich to carbon-rich AGB stars in the LMC acted as constraints to the model.

Several models are calculated to demonstrate the effects of the various parameters. A model with $M_c^{\rm min}=0.58M_\odot$, $\lambda=0.75$, $\eta_{\rm RGB}=0.86$, $\eta_{\rm AGB}=\eta_{\rm EAGB}=5$, including HBB reproduces the observations quite well. It is possible that the amount of carbon formed after a TP is higher than the standard value of $X_{12}=0.22$. As long as $\lambda X_{12}=0.165$ the model fits the observations. It is difficult to discriminate between a higher $X_{12}$ and a higher $\lambda$. Third dredge-up needs to be more efficient and must start at lower core masses than commonly predicted to account for the observed carbon star LF. It is suggested that evolutionary calculations have been performed with mixing-length parameters which are too small.

The adopted mass loss rate coefficients correspond to a pre-AGB mass loss of $0.20M_\odot$ for a $1M_\odot$ and $1.8M_\odot$ for a $5M_\odot$ star. The low mass stars lose this on the RGB, the high mass stars in the core helium burning phase when they reach high luminosities before the TP-AGB. The Reimers coefficient on the AGB ($\eta_{\rm AGB}=5$) corresponds to a mass loss rate of $1.0\ 10^{-6}M_\odot\ {\rm yr}^{-1}$ at the first TP for an initially $1M_\odot$ star with LMC abundances.

These high mass loss rates are necessary to fit the initial–final mass relation and the high luminosity tail of the carbon star LF. The lifetime of the massive stars with these high mass loss rates are in good agreement with the observed number of massive AGB stars and their progenitors, the Cepheid variables. We suggest that the core mass at the first TP for massive stars has previously been overestimated because their evolution was calculated neglecting pre-AGB mass loss.

Observationally the distribution of $^{13}$C enriched carbon stars in the LMC is bimodal. There is a small number ($\sim$0.1%) of high–luminosity ($M_{\rm bol}<-5$) J-type stars and a larger ($\sim$10%) number of low–luminosity ($M_{\rm bol}>-4.75$) J-type stars. The difference in relative numbers as well as the gap in luminosity between the two distributions suggst a different evolutionary origin. The low–luminosity J-type stars may be related to the R-stars in the Galactic bulge which have luminosities between $0\lesssim M_{\rm bol}\lesssim -3$ indicating an origin at luminosities below the AGB.

The small number of high–luminosity J-type carbon stars can be explained by HBB. Given the uncertainty in the observed LF and our approximate treatment of HBB the agreement is good. We predict that about 1% of M and S stars are enriched in $^{13}$C (and $^{14}$N).

We considered the effect of "obscuration", when stars lose so much mass that they become optically invisible. Based on $V$-band, $I$-band and IRAS data of Reid et al. (1990) and a radiative transfer model we find that at most 3% of all carbon stars brighter than $M_{\rm bol}=-6$ could have been missed in optical surveys. Using our model we derive that the overall effect of obscuration of carbon stars is negligible ($\sim$0.1%).

The predicted average final mass ($M_{\rm f}=0.59M_\odot$) is in good agreement with the observed value ($0.60\pm0.02M_\odot$). We predict for our LMC model that stars with initial masses larger than $1.2$–$1.4M_\odot$ turn into carbon stars directly and that stars initially more massive than about $1.5M_\odot$ pass through an intermediate S-star phase before becoming carbon stars. This is consistent with the observation of carbon stars and S-stars in LMC clusters.

The predicted birth rate of AGB stars is found to be in agreement with the death rate of Cepheids and the clump stars.

*Send offprint requests to*: M.A.T. Groenewegen

The birth rate of planetary nebulae (PN) is a factor of 2 lower than the death rate of AGB stars suggesting that low mass stars ($M \lesssim 1.1 M_{\odot}$) may not become PN.

**Key words:** stars: carbon – stars: evolution – stars: late type – stars: mass loss – Magellanic Clouds

## 1. Introduction

Stars in the main sequence mass range $0.9 M_{\odot} \lesssim M_{\rm ms} \lesssim 8 M_{\odot}$ go through a double-shell burning phase, also refered to as the asymptotic giant branch (hereafter simply AGB) phase, at the end of their life. In this phase carbon is dredged up to the surface after each thermal pulse (TP), also referred to as a Helium shell flash, by convective dredge-up. By mixing additional carbon into the envelope a star can be transformed from a M-star phase (oxygen-rich), to a S-star phase (carbon about equal to oxygen) or a C-star phase (carbon outnumbering oxygen).

Although this general principle is well understood (see e.g. the review by Iben & Renzini 1983; hereafter IR) many problems remain. Progress in this field has been slow however because it is very (computer) time consuming to calculate an AGB-model using stellar evolution codes. For example, it takes about 2000 models to calculate one TP and the following interpulse period for one set of parameters. To explore the influence of metallicity or mass loss in this way is a formidable task. Finally, to calculate a consistent AGB-model one would have to evolve it from the main sequence to the red giant phase and to the AGB. A consistent set of models including the latest physics, with a sufficient narrow grid in stellar mass, metallicities and mass loss rates is not available and will probably not be available for some years to come.

To make progress in our understanding of stellar evolution on the AGB it is therefore useful to turn to "synthetic" AGB-evolution. In synthetic evolution one uses empirical laws, derived from "exact" model calculations, to calculate the evolution of an AGB star. The predicted results, e.g. final masses or luminosity functions (LF) can than be compared to observations. This can provide information about quantities such as the mass loss rate on the AGB or the minimum core mass for dredge-up.

The first to use synthetic evolution models for the AGB were Iben & Truran (1978; hereafter IT). They were primarily interested in the abundances of the *s*-process elements. The most well known study is probably that of Renzini & Voli (1981; hereafter RV). Their results were used to compare the theoretical luminosity function of carbon stars with the observed one in the LMC (Frogel et al. 1981; Richer 1981b) and to compare the predicted abundances in the ejecta of the AGB stars with the observed abundances in planetary nebulae (PN) (see Clegg 1991 and references therein). RV also calculated the amount of matter returned to the interstellar medium (ISM) in the form of $^4$He, $^{12}$C, $^{13}$C, $^{14}$N, $^{16}$O, which were used in Galactic chemical evolution models (e.g. Matteucci et al. 1989; Rocca-Volmerange & Schaeffer 1990). Other studies employing synthetic evolution are Scalo & Miller (1979), Iben (1981), IR, Frantsman (1986), Bedijn (1988) and, more recently, de Jong (1990) and Bryan et al. (1990).

Except for the Bryan et al. study, the formulae used in these studies were mainly based on evolutionary AGB calculations for massive stars ($3 \lesssim M/M_{\odot} \lesssim 8$). These results were then extrapolated to less massive stars. This may not be (and indeed is not, as we will discuss later) valid. Another important aspect which was neglected in almost all studies so far, is the metallicity dependence of the evolutionary algorithms used. From observations of the Magellanic Clouds it was derived that the LF of carbon stars is probably different in the LMC and SMC. One of the explanations for this difference is the different metallicity in these systems (see e.g. Lequeux 1990).

In recent years several detailed studies of AGB evolution have been published which concentrate on low mass stars ($0.9 \lesssim M/M_{\odot} \lesssim 3$) and also investigate the metallicity dependence (e.g. Iben 1982; Boothroyd & Sackmann 1988a–d, hereafter BS1, BS2, BS3, BS4; Lattanzio 1986, 1987a, b, 1989a–c; Hollowell 1987, 1988). With these new results it is possible to extend the empirical laws to lower masses as well as to include a metallicity dependence.

An important effect which was not included in most synthetic models is the variation of the luminosity during the flashcycle. During about 20% of the time following a TP the luminosity of the star is about 0.5 magnitude below its pre-flash value. This has significant implications for any theoretical LF since inclusion of this effect will create a significant (low-) luminosity tail in the LF.

Another important fact neglected in most synthetic evolution models so far is that during the first few pulses, when the TPs are not yet at full amplitude, the luminosity is lower than given by the canonical core-mass–luminosity relations. This will also affect the low–luminosity tail of the LF.

The aim of this paper is to present a synthetic evolution model which includes physical effects like the ones described above, and also to include as much as possible the metallicity dependence of all relations used. In Sect. 2 we present the model and in Sect. 3 we apply it to the LMC with emphasis on a comparison with the observed LF of carbon stars in the LMC. The results are discussed in Sect. 4.

## 2. The model

We start with describing the conditions of the star at the first TP. We proceed with the core–mass–luminosity relation for full amplitude pulses, the core–mass–interpulse period relation, the position of a star in the HR-diagram, the mass loss rate before and on the AGB, the effect of the luminosity variations during the flash cycle and finally the effects of the first, second and third dredge-up are discussed.

### 2.1. *Conditions at the first thermal pulse*

Since the evolution of an AGB star is governed by its core mass, the core mass at the first TP [$M_{\rm c}(1)$] is the most important quantity for determining the initial condition of an AGB star. Since the luminosity of a star at the first TP is lower than the luminosity given by the core–mass–luminosity relation for full amplitude pulses (see below) a second important quantity is the luminosity at the first TP [$L(1)$].

#### 2.1.1. The core mass at the first thermal pulse

For low mass stars ($M \leq 3 M_{\odot}$) we use the formulae presented by Lattanzio (1989c). The core mass (in solar units) at the first TP for

low mass stars is given by

$$M_c(1)=\begin{cases}0.53-(1.3+\log Z)(Y-0.2), & Z\geq 0.01,\\ 0.524+0.58(Y-0.2)+[0.025-20Z(Y-0.2)]M, & 0.003\leq Z\leq 0.01,\\ (0.394+0.3\,Y)\exp[M(0.1+0.3\,Y)], & Z\leq 0.003,\end{cases} \quad (1)$$

where $Y$ is the helium content and $Z$ the metallicity at the first TP and $M$ the (initial) mass in solar units.

For higher mass stars, i.e. stars massive enough to undergo the second dredge-up (see Sect. 2.9.3) we use the formalism of RV as originally put forward by Becker & Iben (1970, 1980; hereafter BI1 and BI2). For completeness we will repeat them here.

Define $Z_1=\log(Z/0.02)$, $Z_2=Z-0.02$, $Y_1=\log(Y/0.28)$, $Y_2=Y-0.28$ where $Z$, $Y$ are the main sequence values. The mass of the core just before the second dredge-up is given by

$$M_c^B=AM+B, \quad (2)$$

where

$$A=0.2954+0.0195Z_1+0.377Y_1-1.35Y_1^2+0.289Z_1Y_1,$$

$$B=-0.500-30.6Z_2-412Z_2^2-1.43Y_2+29.3Y_2^2-204Z_2Y_2. \quad (3)$$

The mass of the core just after the second dredge-up is given by

$$M_c^A=CM+D, \quad (4)$$

where

$$C=0.0526+0.754Z_2+54.4Z_2^2+0.222Y_2-1.07Y_2^2+5.53Z_2Y_2,$$

$$D=0.590-10.7Z_2-425Z_2^2-0.825Y_2+9.22Y_2^2-44.9Z_2Y_2. \quad (5)$$

The lowest mass for which the second dredge-up will occur, $M_{crit}$, is determined from $M_c^B=M_c^A$ and is therefore given by

$$M_{crit}=(B-D)/(C-A). \quad (6)$$

Therefore, for stars more massive than $M_{crit}$, the core mass at the first TP equals $M_c^A$. This assumes that there is no significant increase in the core mass between the second dredge-up and the first TP. This is indeed the case as can be verified by comparing Table 4 of BI1 (listing $M_c^A$) and Table 2 of BI2 [listing the true value of $M_c(1)$]. The differences are of the order of $0.001M_\odot$. For stars in the range $3<M/M_\odot<M_{crit}$ we interpolate linear in $M_c(1)$.

In Fig. 1 the core mass at the first TP is plotted as a function of initial mass for the composition $Z=0.02$, $Y=0.28$ (solid line) and $Z=0.001$, $Y=0.24$ (dashed line). For comparison the values of $M_c(1)$ given by BS3 for $Z=0.02$, $Y=0.27$ (circles) and $Z=0.001$, $Y=0.24$ (plusses) and the recent results from Castellani et al. (1990) for $Z=0.02$, $Y=0.27$ (diamonds) are plotted. The dotted line represents the relation used by RV, irrespective of composition, for the low mass stars. In general there is good agreement for the massive stars. For the low mass stars, BS find somewhat lower initial core masses compared to Lattanzio.

### 2.1.2. The luminosity at the first thermal pulse

For low mass stars [$M_c(1)\leq 0.8$] the luminosity (in solar units) at the first TP, $L(1)$, is derived by fitting a straight line to data points in Fig. 4 of BS2:

$$L(1)=\begin{cases}29\,000\ [M_c(1)-0.5]+1000, & Z=0.001,\\ 27\,200\ [M_c(1)-0.5]+1300, & Z=0.02.\end{cases} \quad (7)$$

For other metallicities we interpolated in log $Z$.

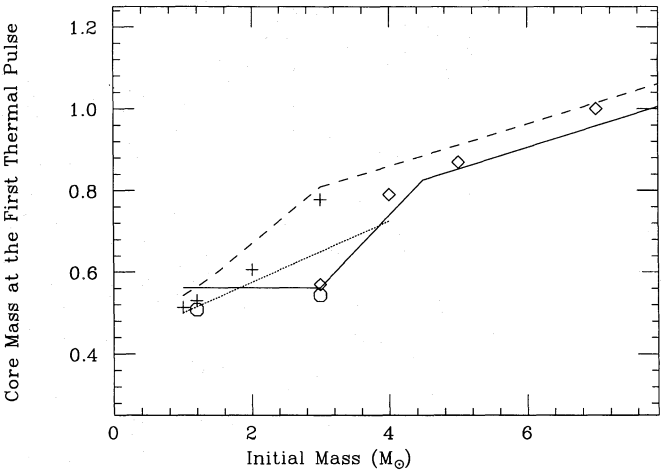


**Fig. 1.** The core mass at the first thermal pulse, $M_c(1)$, derived from Eqs. (1) and (4) for the composition $Z=0.02$, $Y=0.28$ (solid line) and $Z=0.001$, $Y=0.24$ (dashed line). The standard pre-AGB mass loss rate of Sect. 2.6.1 was used to calculate $M_c(1)$. For comparison the results of BS3 for $Z=0.02$, $Y=0.27$ (circles) and $Z=0.001$, $Y=0.24$ (plusses) and of Castellani et al. (1990) for $Z=0.02$, $Y=0.27$ (diamonds) are also plotted. The dotted line represents the formula used by RV, irrespective of composition, for the low mass stars

For massive stars [$M_c(1)\geq 0.85$] we reexamined the original data presented by BI1 (their Table 2). Following the suggestion of BS2 that the composition dependence of the core–mass–luminosity relation for full amplitude pulses for low mass stars scales with $\mu^3$, where $\mu$ is the mean molecular weight,

$$\mu=\frac{4}{5X+3-Z}, \quad (8)$$

we included a $\mu^a$ term in our fit to the BI data. Our result,

$$L(1)=213\,180\ \mu^2\ [M_c(1)-0.638], \quad (9)$$

gives a surprisingly good fit (within 5%) to all the datapoints, given the wide range of metallicities ($0.001<Z<0.03$) and helium contents ($0.20<Y<0.36$) considered by BI. The luminosities derived with Eq. (9) agree to within 5% with those recently reported by Castellani et al. (1990). The fact that the $\mu$ dependence for high mass stars is weaker than for low mass stars was predicted by Kippenhahn (1981) based on earlier work of Refsdal & Weigert (1970). For stars in the range $0.8\leq M_c(1)\leq 0.85$ we interpolate between Eqs. (7) and (9).

### *2.2. The interpulse period and luminosity for full amplitude pulses*

For AGB stars in which the pulses have reached full amplitude there exist some very useful relations discovered by Paczynski

(1970, 1975): the core–mass–luminosity and the core–mass–interpulse period relation respectively.

#### 2.2.1. The core–mass–luminosity relation

For the low mass stars ($M_c < 0.7$) we use the core–mass–luminosity relation derived and presented in BS2:

$$L = 238\,000\ \mu^3\ Z_{cno}^{0.04}\,(M_c^2 - 0.0305\,M_c - 0.1802), \quad (10)$$

where $Z_{cno}$ is the total abundance of carbon, nitrogen and oxygen ($Z_{cno}$ is roughly $0.6\,Z$) and $\mu$ is the same as in Eq. (8). All luminosities in this paper are in solar units.

For high mass stars ($M_c > 0.95$) we modified the equation presented by IT (see also Iben 1977),

$$L = 63\,400\ (M_c - 0.44)(M/7)^{0.19},$$

in the following manner. Iben presented his formula for a mixing-length parameter $\alpha = 1/H_p = 0.7$. BS2 argue that Iben's definition of $\alpha$ is different from the common one and his value corresponds to $\alpha \approx 1.3$ in most other models. But even this value for $\alpha$ is lower than presently felt to be the appropriate value, $\alpha \approx 1.9$ (Maeder & Meynet 1989). Iben reported an increase in luminosity by 15% if $\alpha$ is increased from 0.7 to 1.0. We took the luminosities at different core masses reported by Iben (1977) for his $M = 7M_\odot$ model and increased them by 15% to simulate the more appropriate value of $\alpha$. We then fitted a straight line to it. We kept the mass dependence given by IT and introduced a composition dependence. For the composition dependence we assumed $L \sim \mu^2$, simply because this gave very good results for the $L$–$M_c(1)$ relation for massive stars (see Sect. 2.1.2). This assumption is not of any practical importance because $\mu$ changes only by 4% when $Z$ is changed from 0.005 to 0.02 and $Y$ is chosen according to Eq. (24). Our final result for the higher mass stars is

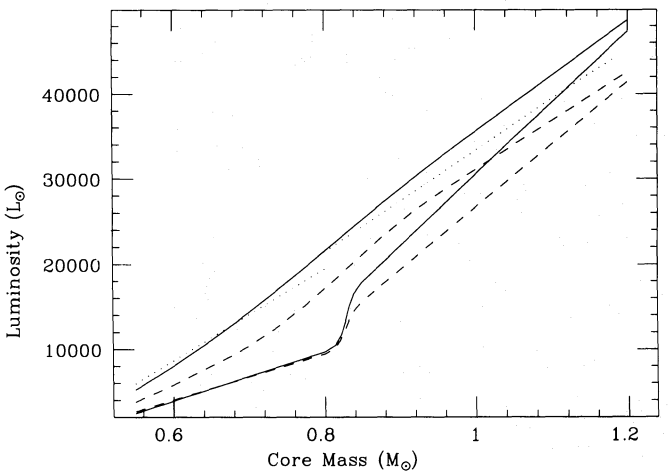


**Fig. 2.** The core–mass–luminosity relations for the first TP (lower solid and dashed curves) and for full amplitude pulses (upper solid and dashed curves) used in this work. Indicated are $Z = 0.02$ (solid line) and $Z = 0.001$ (dashed line). Note the difference between the luminosity at the first thermal pulse and for full amplitude pulses, especially for low core masses. For comparison, the dotted curve is the relation used by RV, irrespective of metallicity and pulse number. The lower part ($M_c \leq 0.8M_\odot$) of this curve was calculated for a $M = 3M_\odot$, the upper part for a $M = 5M_\odot$ star. The wiggle in the relations for the luminosity at the first TP is due to the joining of Eq. (7) with Eq. (9)

$$L = 122585\ \mu^2\ (M_c - 0.46)\ M^{0.19}. \quad (11)$$

For stars with $0.7 < M_c < 0.95$ we interpolate between Eqs. (10) and (11).

Recent calculations by Blöcker & Schönberner (1991) seem to indicate that the standard core–mass–luminosity relation may not be valid in the case of the massive stars. We have not taken this effect into account. Their results depend sensitively on the adopted mixing length parameter. Since they use the Cox & Steward (1970) opacities, their choice for the mixing length parameter is rather high ($\alpha = 2$). Furthermore, when the evolution of this model is continued, the luminosities fall on the standard core–mass–luminosity relation again (Schönberner 1991).

In Fig. 2 the core–mass–luminosity relations for both full amplitude pulses and at the first TP for both $Z = 0.02$ and 0.001 are shown. The helium abundance was calculated from Eq. (24) and the luminosity for the high core–masses was calculated for $M = 5M_\odot$. The difference in luminosity due to the difference in metallicity is about 0.4 in bolometric magnitude. Figure 2 shows that it is important to take into account that during the first few pulses the luminosity is below the value given for full amplitude pulses. The difference can amount to 0.8 magnitudes. For comparison the core–mass–luminosity relation used by RV, irrespective of metallicity or pulse number, for a $M = 3M_\odot$ and a $M = 5M_\odot$ star, is also plotted.

#### 2.2.2. The core–mass–interpulse period relation

The timescale on which TPs occur is a function of core mass as was discovered by Paczynski (1975). For all core masses we use the core–mass–interpulse period relation presented in BS3:

$$\log t_{ip} = \begin{cases} 4.50\ (1.689 - M_c), & Z = 0.02, \\ 4.95\ (1.644 - M_c), & Z = 0.001. \end{cases} \quad (12)$$

For other metallicities we interpolated in $\log t_{ip}$ using $\log Z$ as variable. The interpulse period is expressed in years. Both equations are derived for $M_c < 0.85$, but since Eq. (12a) is almost identical to the original Paczynski relation, $\log t_{ip} = 4.5\,(1.678 - M_c)$, which is valid in the range $0.5 \lesssim M_c \lesssim 1.4$ and for $Z = 0.03$, it seems justified to extend Eq. (12a) to all core masses. For the low metallicity case there seems to be no data available regarding the $M_c$–$t_{ip}$ relation for high mass stars, so we assume Eq. (12b) to be valid over the whole range of core masses. In actual computations this assumption will not play a significant role because high core masses are attained only by high mass stars which, in general, have a metallicity closer to $Z = 0.02$ than to $Z = 0.001$, even in the LMC.

In Fig. 3 the interpulse period is shown for $Z = 0.02$ and 0.001. For comparison the interpulse period relation derived from the formulae in RV for a $1M_\odot$ star with $Z = 0.001$ and a $5M_\odot$ star with $Z = 0.02$ (the dotted lines) are also shown. The differences with the formulae of BS are large for the lowest core masses. The formulae used by RV (taken from Iben 1977) were derived for $M_c \gtrsim 0.65$. In this region the old and new formula agree reasonably.

### *2.3. From the first pulse to full amplitude pulses*

It has been long known (see IR for references) that it takes some time before the thermal pulses reach full amplitude. During this period the equations presented in Sects. 2.2.1 and 2.2.2 are not

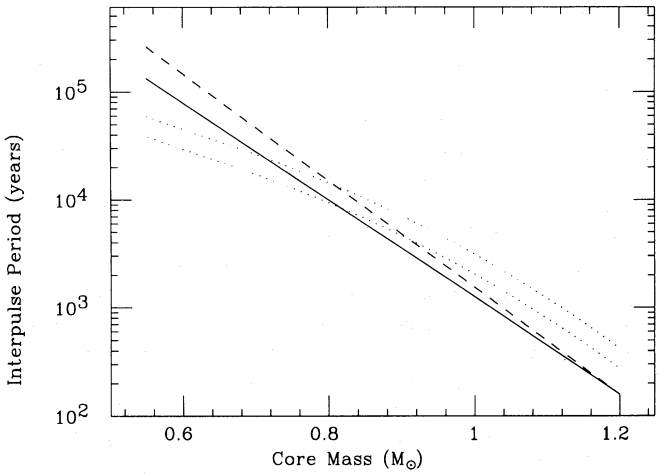


**Fig. 3.** The core–mass–interpulse period relations for $Z=0.02$ (solid line) and $Z=0.001$ (dashed line) used in this work. The interpulse period is significantly larger for low metallicities. For comparison the interpulse periods calculated from the formulae of RV for a star of $M=1M_\odot$ and $Z=0.001$ (upper dotted line) and $M=5M_\odot$ and $Z=0.02$ (lower dotted line) are also shown. Differences with the more recent relations are large, especially for low core masses. This emphasizes, that formulae which were derived for high core masses, as the one of RV, cannot be arbitrarily extrapolated to low core masses

applicable, without proper corrections. Since these corrections are necessary during approximately the first half dozen pulses they will mainly affect the low mass stars; a $1.5M_\odot$ star experiences about 50 TP, a $4M_\odot$ star about 1000 pulses during its AGB phase (RV).

2.3.1. Corrections to the core–mass–luminosity relation

From the data presented in Fig. 4 of BS2 we deduce that it takes approximately 6 flashes before the luminosity at a given core mass lies on the core–mass–luminosity relation for full amplitude pulses. This agrees with other calculations (e.g. Wood & Zarro 1981; Lattanzio 1986).

We introduce a correction factor, $f$, depending upon the time already spent on the AGB, by which the luminosity, obtained from Eqs. (10) or (11), has to be multiplied to approximately get the true luminosity. For $f$ a simple linear relation is assumed:

$$f=f_1+(1-f_1)t/\tau \quad (t\leq\tau), \tag{13}$$

where $t$ is the time spent on the AGB and $\tau$ is the time at which the TPs have reached full amplitude. We have taken $\tau$ to be 6 times the interpulse period at the first TP. For the first TP we have $f=f_1$, and so $f_1$ can be derived from

$$f_1=L(1)/L. \tag{14}$$

Typical values for $f_1$ are 0.55 for a $1M_\odot$ star with $Z=0.005$ and 0.67 for a $4.5M_\odot$ star with $Z=0.02$.

**Table 1.** The correction factors $\Delta M_c$ for the interpulse period during the first six pulses

| Pulse number | $\Delta M_c$ | |
|---|---|---|
| $N_p$ | $Z=0.02$ | $Z=0.001$ |
| 1 | 0.09 | 0.06 |
| 2 | 0.065 | 0.01 |
| 3 | 0.04 | 0 |
| 4 | 0.03 | 0 |
| 5 | 0.02 | 0 |
| 6 | 0.01 | 0 |
| ≥7 | 0 | 0 |

2.3.2. Corrections to the core–mass–interpulse period relation

From Fig. 11 in BS3 we derive that during the first few pulses the interpulse period is much shorter compared to the values given by the Eqs. in 2.2.2. It seems that the star mimics a star of higher core mass.

In order to approximately get the correct interpulse period during the first six pulses we introduce a correction factor, $\Delta M_c$, which has to be added to the true core mass to get an "effective" core mass to be used in Eq. (12). The correction factors $\Delta M_c$ are given in Table 1.

*2.4. The HR diagram*

To obtain the position of a star in the Herzsprung–Russell diagram we need to link the luminosity of a star to its effective temperature ($T_{\rm eff}$ in Kelvin).

We use the relations presented by Wood (1990) derived for oxygen-rich Miras:

$$\log T_{\rm eff}=\begin{cases}(M_{\rm bol}+59.1+2.65\log M)/15.7-0.12\ \log(Z/0.02)+\Delta & (M\leq 1.5),\\ (M_{\rm bol}+74.1+4.00\log M)/20.0-0.10\ \log(Z/0.02) & (M\leq 2.5),\end{cases} \tag{15}$$

where $M_{\rm bol}=-2.5\log L+4.72$ and $\Delta$ is a correction term which accounts for the fact that the effective temperature increases at the end of the AGB when the envelope mass becomes small. The $\Delta$ term is calculated from Wood (1990):

$$\Delta=\begin{cases}0, & x\geq 0.8,\\ 0.07\ (0.8-x)^{2.54}, & x<0.8,\end{cases} \tag{16}$$
$$x=M_{\rm bol}+7.0-1.2/M^{1.7}.$$

For intermediate mass stars we interpolate in $\log T_{\rm eff}$ using the mass $M$ as variable. The zero point of these relations was determined by Wood from the assumption that the star o Ceti (Mira) with a period of 330 d, $Z=Z_\odot$, $M_{\rm bol}=-4.32$, has a mass of $1M_\odot$ and is pulsating in the fundamental mode. If o Ceti has a mass of $2M_\odot$ or is a first overtone pulsator the zero point in Eq. (15a) would be 57.1. This translates into a difference in $T_{\rm eff}$ of 15%.

The radius of the star (in solar units) is derived from

$$R=\sqrt{\frac{L}{(T_{\rm eff}/5770)^4}}. \tag{17}$$

Equation (15) is, strictly speaking, only valid for oxygen-rich stars, but we also used it for carbon stars, lacking any better estimate. If the $T_{\rm eff}$–$L$ relation would be different for carbon stars this would merely affect the choice of the mass loss scaling parameter $\eta_{\rm AGB}$ (Sect. 2.6.2), through the dependence of the mass loss rate on the stellar radius and hence on the effective temperature.

### 2.5. The rate of evolution

Since hydrogen burning is the source of energy during most of the interpulse period, the rate of evolution, i.e. the rate of core mass growth in $M_\odot\,{\rm yr}^{-1}$ is to a good approximation given by

$$\frac{{\rm d}M_{\rm c}}{{\rm d}t}=9.555\ 10^{-12}\frac{L_{\rm H}}{X}, \tag{18}$$

where $X$ is the hydrogen abundance (by mass) in the envelope, $L_{\rm H}$ the luminosity provided by H-burning (in solar units) and the numerical factor includes the energy released from the burning of 1 g of hydrogen ($6.4\ 10^{18}$ erg).

There is a small contribution from He-burning and gravitational energy to the total luminosity $L$, so that

$$L=L_{\rm H}+2000(M/7)^{0.4}\exp[3.45(M_{\rm c}-0.96)]. \tag{19}$$

This equation, derived for high mass ($M_{\rm c}>0.96$) stars, is taken from IT (see also RV) but we changed the exponent of the mass dependence from 0.19 to 0.4. This has no significant influence for high mass stars but gives better results when compared to the value given by Paczynski (1970) for a star with a core mass of $0.57M_\odot$. The correction to the total luminosity due to He-burning and gravitational energy is small: for a $M=7M_\odot$ star with $M_{\rm c}=0.96$ it is 6%, for a $M=1M_\odot$ star with $M_{\rm c}=0.6$ the correction term equals 4% of the total luminosity.

### 2.6. The mass loss process

The mass loss process on the AGB (but also prior to this phase) is an important, but unfortunately, a poorly understood phenomenon. The mass loss rate on the AGB has important consequences for the evolution of a star. It reduces the envelope mass more rapidly with the effect that (a) AGB evolution is terminated at a lower core mass, i.e. luminosity, (b) a star is more easily turned into a carbon star since less carbon needs to be dredged up and (c) it hampers the dredge-up process (Wood 1981).

The mass loss rate on the AGB has also important consequences with regard to the LF function derived for e.g. carbon stars in extragalactic systems. With the advent of the IRAS satellite it has become clear that there exist many sources in our galaxy (e.g. OH/IR sources or obscured carbon stars) which lose mass at such a rate ($>10^{-5}M_\odot\,{\rm yr}^{-1}$) that they are optically very faint or even invisible. Their IR-signature (silicate emission or absorption, silicon carbide or amorphous carbon emission) is an important diagnostic to identify these sources as either oxygen- or carbon-rich. Since the identification of carbon stars in extragalactic systems is done using the $C_2$ bands at 4735 and 5165 Å or the CN bands at 7945, 8125, 8320 Å or $V$, $R$, $I$ filters (see e.g. Lequeux 1990) these surveys could easily have missed carbon stars with optically thick dust shells. The IR surveys carried out so far (see e.g. Frogel & Richer 1983) did not go deep enough to detect these dust enshrouded stars, if they exist. Since stars with thick dust shells are usually associated with somewhat more luminous stars this implies that the LF presented for carbon stars (and also for M-stars) in extragalactic systems might be incomplete at the high luminosity end. To investigate the existence, and relative importance, of obscured stars we calculated the LF of stars below and above a critical value of the mass loss rate, $\dot{M}_{\rm IR}$, to simulate optical visible and obscured stars. Details are given in Appendix C.

#### 2.6.1. Mass loss up to the AGB

For low mass stars, i.e. stars which undergo the helium core flash (HeCF), the most important phase prior to the AGB regarding mass loss is the red giant branch (RGB). Several tenths of solar masses can be lost in this phase.

We parametrised the values of the mass loss on the RGB from the data presented in Fig. 8 of Sweigart et al. (1990). From this it is deduced that the amount of mass lost on the RGB, $\Delta M$, is well represented by two straight lines,

$$\Delta M=\begin{cases} A_1M+B_1, & M<M_1,\\ A_2M+B_2, & M_1\le M<M_2,\\ 0, & M\ge M_2,\end{cases} \tag{20}$$

$M$ being the initial mass. The coefficients $A_1$, $A_2$, $B_1$, $B_2$ as well as $M_1$ and $M_2$ are listed in Table 2. We interpolate linearly in $\Delta M$ using $Y$ and $\log Z$ as variables. The values given by Sweigart et al. (1990) are calculated for $\eta_{\rm RGB}=2/3$ ($\eta_{\rm RGB}$ being the coefficient in the Reimers law). For any other desired value of $\eta_{\rm RGB}$ one has to multiply the values calculated with Eq. (20) with an appropriate factor.

It is interesting to note that the amount of mass lost on the RGB increases with decreasing mass. This is due to two effects. Firstly, the luminosity at the tip of the RGB increases with

**Table 2.** The amount of mass loss on the RGB

| Composition | | $A_1$ | $B_1$ | $M_1$ | $A_2$ | $B_2$ | $M_2$ |
|---|---|---|---|---|---|---|---|
| $Y=0.2$ | $Z=0.004$ | −0.108 | 0.300 | 2.10 | −0.292 | 0.689 | 2.36 |
| | 0.010 | −0.106 | 0.317 | 2.20 | −0.250 | 0.625 | 2.50 |
| | 0.040 | −0.104 | 0.339 | 2.25 | −0.160 | 0.465 | 2.91 |
| $Y=0.3$ | $Z=0.004$ | −0.116 | 0.269 | 1.77 | −0.224 | 0.467 | 2.08 |
| | 0.010 | −0.124 | 0.306 | 1.85 | −0.232 | 0.506 | 2.18 |
| | 0.040 | −0.132 | 0.348 | 2.00 | −0.168 | 0.420 | 2.50 |

*Note*: The coefficients $A_1, A_2, B_1, B_2, M_1, M_2$ refer to Eq. (20).

decreasing mass in the mass range $M_1 \lesssim M \lesssim M_2$ (see e.g. Fig. 2 of Sweigart et al. 1990). Secondly, the time spent between the main sequence and the tip of the RGB increases with decreasing mass (see e.g. Sweigart et al. 1989). This means that $\Delta M \sim \dot{M}\,\Delta t \sim L\,\Delta t$ increases with decreasing mass.

For stars which do not pass through the HeCF the amount of matter lost on the RGB is negligible. For a $3M_\odot$ star ($Z=0.02$, $Y=0.27$) BS3 finds that $\Delta M = 0.003 M_\odot$, even for $\eta_{\rm RGB}=1.4$. So the fact that we assume $\Delta M = 0$ for $M \geq M_2$ is justified.

The most appropriate value of $\eta_{\rm RGB}$ can be derived from the observational constraint that population II stars on the horizontal branch must have lost approximately $0.2M_\odot$ on the RGB (Rood 1973). Specifically, if we take Rood's model for M 3 that a $M=0.85M_\odot$ star with $X=0.75$ and $Z=0.017$ has lost $0.22M_\odot$ on the RGB, the appropriate value for $\eta_{\rm RGB}$ using the mass loss rates from the models of Sweigart et al. is $\eta_{\rm RGB}=0.86$. This will be our prime choice for $\eta_{\rm RGB}$ in our models.

Massive stars evolve up to high luminosities before they experience their first TP (see Fig. 2). If Reimers law is still applicable, massive stars can lose a considerable amount of mass before the first TP on the horizontal branch (HB) and early-AGB. We parametrized the results of Maeder & Meynet (1989) for stars in the range $3$–$7M_\odot$ and find for the mass lost up to the first TP for the massive stars (in solar units):

$$\Delta M_{\rm EAGB} = \eta_{\rm EAGB}\ 0.056\ (M/3)^{3.7}. \quad (21)$$

The subscript EAGB stands for early-AGB, although the mass is lost not only on the E-AGB but also on the latest phases of the HB. Maeder & Meynet (1989) use a Reimers law with $\eta_{\rm EAGB}=0.5$, but it is not clear if this value is appropriate because the mass loss rates of stars are on the E-AGB are unknown.

#### 2.6.2. Mass loss on the AGB

Mass loss on the AGB will be represented by Reimers (1975) law:

$$\dot{M} = \eta_{\rm AGB}\ 4.0\ 10^{-13}\ \frac{LR}{M}\quad M_\odot\,{\rm yr}^{-1}. \quad (22)$$

The luminosity $L$ is not the quiescent luminosity but includes the effect of the luminosity variation during the flashcycle, i.e. the mass loss rate just after a TP is higher than at quiesence or in the luminosity dip. We do not include an explicit metallicity dependent term in the mass loss rate, as for example is suggested from the study of the mass loss rates of hot O-stars in the Galaxy and the Magellanic Clouds which seem to indicate $\dot{M} \sim Z^{0.5}$ (Kudritzki et al. 1987).

From IR's relation between $\eta$ and the final mass it is derived that $\eta_{\rm AGB} \gtrsim 3$ is needed to fit the observed initial–final mass relation in the Galaxy (see Weidemann & Koester 1983). Therefore the initial value in our model will be $\eta_{\rm AGB}=3$.

### 2.7. *When to end the AGB evolution?*

Basically two approaches have been adopted to this question. The first approach is to end the AGB evolution with the instantaneous ejection of what is supposed to represent a planetary nebulae (PN). This solution has been adopted by de Jong (1990), who assumed that 10% of the initial mass was ejected at the end of the AGB, as well as RV who assumed a core mass dependent relation [their Eq. (33)] which increases from $0.02\,M_\odot$ at $M_{\rm c}=0.5M_\odot$ to a maximum of $1.38M_\odot$ at $M_{\rm c}=1.33M_\odot$.

The second approach is to end the evolution on the AGB when the envelope mass is reduced below a critical value, when the star starts moving to the left in the HR diagram. This approach is adopted in this study and we used Iben's (1985) suggestion that the critical envelope mass, $M_{\rm end}$, is given by

$$M_{\rm end} = 0.1\,\frac{{\rm d}M_{\rm c}}{{\rm d}t}\,t_{\rm ip}. \quad (23)$$

For typical parameters this corresponds to $M_{\rm end}=7.9\ 10^{-4}M_\odot$ ($M_{\rm c}=0.6M_\odot$, $M=1.5M_\odot$, $X=0.7$, $Z=0.02$) or $M_{\rm end}=9.4\ 10^{-6}$ $M_\odot$ ($M_{\rm c}=1.2M_\odot$, $M=7M_\odot$, $X=0.7$, $Z=0.02$). For lower metallicities, $M_{\rm end}$ increases due to the increase in the interpulse period. For the $M=1.5M_\odot$ star e.g., $M_{\rm end}=1.3\ 10^{-3}M_\odot$ when $Z=0.001$. These values agree within a factor two with the formula given by Iben (1985), the difference probably being due to differences in total mass and composition. The values of $M_{\rm end}$ derived here also agree with the values reported by Paczynski (1971), Schönberner (1983) and Blöcker & Schönberner (1990).

### 2.8. *The flashcycle*

The luminosity between two thermal pulses is not constant (as given by the equations in Sect. 2.2.1). It has been known for a long time (see e.g. IR) that for short periods of time the luminosity can be both higher and lower than the quiescent value.

From the data presented by BS1 as well as from Iben (1975), Sackmann (1980), Wood & Zarro (1981), Iben (1982) and Lattanzio (1986) the following (simplified) relations were derived.

Stars with $M_{\rm env} \leq 2M_\odot$ have, for a brief moment directly following a TP, a luminosity higher than the quiescent value. The duration $t_{\rm flash}$ (in units of the interpulse period, not in years!) and the value $\Delta\log L_{\rm flash}$ to be added to the logarithm of the quiescent luminosity to obtain the peak flash luminosity are given in Table 3. From BS1 these values were found to be slightly metallicity dependent.

More significant is the luminosity dip following this peak, or in the case of high mass stars directly following a TP. The

**Table 3.** The peak luminosity and duration of the flash for stars with $M_{\rm env} \leq 2M_\odot$

| $Z$ | $t_{\rm flash}$ | $\Delta\log L_{\rm flash}$ |
|---|---|---|
| $Z \leq 0.001$ | 0.008 | 0.3 |
| $0.001 < Z \leq 0.02$ | 0.01 | 0.25 |
| $Z > 0.02$ | 0.015 | 0.2 |

*Note*: $t_{\rm flash}$ is relative to the interpulse period.

**Table 4.** The extent of the luminosity dip and its duration

| $M_{\rm env}$ | $t_{\rm dip}$ | $\Delta\log L_{\rm dip}$ |
|---|---|---|
| $M_{\rm env} \leq 0.05$ | 0.4 | − 0.4 |
| $0.05 < M_{\rm env} \leq 0.5$ | 0.3 | − 0.3 |
| $0.5 < M_{\rm env} \leq 1.5$ | 0.25 | − 0.25 |
| $M_{\rm env} > 1.5$ | 0.2 | − 0.2 |

*Note*: $t_{\rm dip}$ is relative to the interpulse period.

duration, $t_{dip}$ (relative to the interpulse period) and the extent of the luminosity dip $\Delta\log L_{dip}$ are given in Table 4. Both parameters depend on the envelope mass. Since large envelopes more easily absorb the changes taking place deep in the star, the duration and extent of the luminosity dip are smaller when the envelope mass is higher.

The shape of the luminosity flash and dip is assumed to be simply rectangular.

### *2.9. First, second and third dredge-up*

One of the fascinating aspects of AGB evolution is the possibility of forming carbon-rich stars by the dredge-up of carbon from the carbon-rich pocket formed after the helium shell flash. This process is generally referred to as third dredge-up.

Before reaching this interesting phase, the main sequence composition has changed during the first dredge-up (experienced by all stars on the RGB) and the second dredge-up (experienced by stars with $M > M_{crit}$; see Sect 2.2.1) occurring on the E-AGB.

In the following sections our treatment of first, second and third dredge-up are described.

#### 2.9.1. The initial composition

The main sequence composition is determined in the following way. The parameter to be specified is the metallicity $Z$. The helium abundance is calculated from

$$Y = Y_0 + \frac{\Delta Y}{\Delta Z} Z. \tag{24}$$

The hydrogen content is calculated from $X = 1 - Y - Z$. We assumed a primordal heium abundance $Y_0$ of 0.231 (Steigman et al. 1989). For the Galaxy values between 1.7 and 5 are quoted for $\Delta Y/\Delta Z$ (Steigman 1985; Pagel et al. 1986). For the LMC and SMC there seems to be no independent estimates. Based on the observed abundances H II regions and field F-type supergiants in the LMC and SMC (Russell & Dopita 1990) we derive that $\Delta Y/\Delta Z = 2.5$ describes the present day abundances well in both LMC and SMC. Since this value is within the quoted range for the Galaxy we will use $\Delta Y/\Delta Z = 2.5$ for Galaxy, LMC and SMC alike.

Following Anders & Grevesse (1989) and Grevesse (1991) the main sequence abundances of carbon, nitrogen and oxygen are chosen as

$$\begin{aligned} Z_{cno} &= 0.791 Z, \\ {}^{12}C &= 0.2384 Z_{cno}, \\ {}^{13}C &= 0.0029 Z_{cno}, \\ {}^{14}N &= 0.0707 Z_{cno}, \\ {}^{16}O &= 0.6880 Z_{cno}. \end{aligned} \tag{25}$$

This implies an initial value $^{12}C/^{13}C = 89$ (all abundances are mass fractions, all ratios will be number ratios, unless otherwise specified). Equation (25) is based on relative solar abundances. Abundance analyses of field stars in the LMC and SMC (Spite & Spite 1991a, b; Barbuy et al. 1991) generally give near solar relative abundances so that Eq. (25) can be used with some confidence for Galaxy, LMC and SMC alike.

#### 2.9.2. The first dredge-up

The first dredge-up occurs when the convective envelope moves inwards as a star becomes a red giant for the first time. The convective motion dredges up material which was previously located near the hydrogen burning shell. Helium and CNO-processed material are brought to the surface.

The treatment of the first dredge-up follows that of RV, except that we changed the numerical values slightly to incorporate the results of Sweigart et al. (1989, 1990).

The increase in the helium abundance, $\Delta Y$, is given by Sweigart et al. (1990). The following fits are based on their results:

$$\Delta Y = \begin{cases} -0.0170\, M_{in} + 0.0425, & M_{in} < 2,\ Y = 0.3, \\ -0.0068\, M_{in} + 0.0221, & 2 \le M_{in} < 3.25,\ Y = 0.3, \\ -0.0220\, M_{in} + 0.0605, & M_{in} < 2.2,\ Y = 0.2, \\ -0.0078\, M_{in} + 0.0293, & 2.2 \le M_{in} < 3.75,\ Y = 0.2, \\ 0, & \text{else.} \end{cases} \tag{26}$$

The small dependence of $\Delta Y$ on $Z$ for a given $Y$ is neglected. The change in hydrogen is opposite to the change in helium:

$$\Delta X = -\Delta Y. \tag{27}$$

The change in $^{12}C$ and $^{14}N$ is calculated from

$$\begin{aligned} g &= \begin{cases} 0.64 - 0.05(M-3), & M < 3, \\ 0.64, & M \ge 3, \end{cases} \\ \Delta^{12}C &= {}^{12}C(g-1), \\ \Delta^{14}N &= -1.167\, \Delta^{12}C, \\ \Delta^{16}O &= -0.01\ {}^{16}O. \end{aligned} \tag{28}$$

The number ratio $^{12}C/^{13}C$ after the first dredge-up does not vary much with mass or composition (Sweigart et al. 1989) and is set to 23.

It should be noted that observations indicate that some stars do not obey the standard model predictions. In particular, the $^{12}C/^{13}C$ ratio after the first dredge-up is often lower than predicted in stars of low mass, down to $^{12}C/^{13}C \approx 10$ (see e.g. the review by Lambert 1991). Rotationally induced mixing may play a role.

#### 2.9.3. The second dredge-up

The second dredge-up is related to the formation of the electron-degenerate CO core in more massive [$M > M_{crit}$, Eq. (6)] stars after central helium exhaustion. The base of the convective envelope moves inward through matter pushed outwards by the He-burning shell.

The treatment of the second dredge-up follows that of RV closely (see also IT and IR). The abundances after the second dredge-up can be obtained from the abundances prior to the second dredge-up and the abundances of the material that is dredged up using the relation

$$X^{after} = a X^{prior} + b X^{du}. \tag{29}$$

The coefficients $a$ and $b$ are as follows:

$$\begin{aligned} a &= \frac{M - M_c^B}{M - M_c^A}, \\ b &= \frac{M_c^B - M_c^A}{M - M_c^A}, \end{aligned} \tag{30}$$

where $M$ is the total mass and $M_c^A$ and $M_c^B$ are calculated from Eqs. (2) and (4). The abundances prior to the second dredge-up are known, and the abundances of the dredged up material are given by RV and IT:

$$Y^{du} = 1 - Z,$$
$$^{14}N^{du} = 14(^{12}C/12 + ^{13}C/13 + ^{14}N/14 + ^{16}O/16),$$
$$^{12}C^{du} = ^{13}C^{du} = ^{16}O^{du} = 0. \quad (31)$$

In the model, Eq. (29) was not used to calculate the hydrogen abundance after the second dredge-up, but was calculated from $X = 1 - Y - Z$, with $Y$ and $Z$ the helium and metal abundance after second dredge-up. This was done to ensure that $X + Y + Z \equiv 1$ at all times.

### 2.9.4. The third dredge-up

Although the third dredge-up is of crucial importance for the formation of carbon stars, it is still poorly understood. There is much debate whether or not material is dredged up at every pulse, and how much. It also seems possible that the dredge-up process is turned off again when a star has become a carbon star (BS4; Lattanzio 1989a).

Another effect which has to be taken into account is the possible destruction of newly dredged up carbon at the base of the convective envelope in the CNO-cycle, a process referred to as hot bottom burning (HBB), and extensively discussed in RV. This process is able to slow down or even prevent the formation of carbon stars. Since $^{12}C$ is processed into $^{13}C$ and $^{14}N$, it also gives rise to the formation of $^{13}C$-rich carbon stars (usually referred to as J-type carbon stars) and $^{14}N$-rich objects. RV treated HBB in considerable detail as a function of the mixing length parameter (they considered $\alpha = 0$, 1.0, 1.5, 2). Because the detailed envelope calculations performed by RV are beyond the scope of this paper and since RV found that the results are sensitive to the unknown mixing length parameter, we decided to include HBB in our model in an approximate way.

In our simple model to describe HBB four parameters are needed: (1) the (average) temperature at the base of the convective envelope, $T_B$, as a function of core and total mass, (2) the fraction ($f_{HBB}$) of newly dredged up matter exposed to the high temperatures at the bottom of the envelope, (3) the amount of matter in the envelope, relative to the total envelope mass, which is mixed down and processed at the bottom of the envelope ($f_{bur}$) and (4) the (average) exposure time, $t_{HBB}$, of matter in the zone of HBB. The value of $T_B$ can be derived from the data presented in RV. We implemented the algorithms used by RV in our code and found good agreement with RV in the case of no HBB for a small change in their quoted parameters. In the case of HBB we derived $f_{bur}$, $f_{HBB}$ and $t_{HBB}$ from fitting our model to the $\alpha = 2$ case of RV. Details are given in Appendix A.

Let us now present the formulae used to describe the third dredge-up process in detail.

It is assumed that there is dredge-up only when the core mass is higher than a critical value $M_c^{min}$. The exact value of $M_c^{min}$ is still a matter of debate. To make headway we initially assume the value of Lattanzio (1989c):

$$M_c^{min} = 0.62 + 0.7\,(Y - 0.20). \quad (32)$$

In Sect. 3 we will investigate if this value of $M_c^{min}$ is compatible with the observed LF of carbon stars in the LMC.

The increase in core mass during the interpulse period is given by

$$\Delta M_c = \int_0^{t_{ip}} \frac{dM_c}{dt}\,dt. \quad (33)$$

A certain fraction of this amount is assumed to be dredged up:

$$\Delta M_{dredge} = \lambda \Delta M_c. \quad (34)$$

The free parameter, $\lambda$, is as a first approach assumed to be constant and is of the order of 1/3 (see e.g. Lattanzio 1989c). Fitting their synthetic models to observations Bryan et al. (1990) found a best fit for $\lambda \approx 0.28$.

The composition of the material formed in the pocket after a TP is assumed to be (BS3): $X_{12} = 0.22$ (carbon), $X_{16} = 0.02$ (oxygen) and $X_4 = 0.76$ (helium). The carbon is formed through incomplete helium burning in the triple $\alpha$ process and the oxygen in the $^{12}C(\alpha,\gamma)^{16}O$ reaction.

Since HBB may be effective, this is not necessarily the composition of the material added to the envelope. If $f_{HBB}$ represents the fraction of the dredged up material processed in the CNO cycle at the bottom of the envelope (as defined above), the amount of material added to the envelope is

$$\Delta^4He = X_4\,\Delta M_{dredge},$$
$$\Delta^{12}C = \left[(1 - f_{HBB})X_{12} + \frac{f_{HBB}}{t_{HBB}} \int_0^{t_{HBB}} X_{12}^{HBB}(t)\,dt\right] \Delta M_{dredge},$$
$$\Delta^{13}C = \left[\frac{f_{HBB}}{t_{HBB}} \int_0^{t_{HBB}} X_{13}^{HBB}(t)\,dt\right] \Delta M_{dredge},$$
$$\Delta^{14}N = \left[\frac{f_{HBB}}{t_{HBB}} \int_0^{t_{HBB}} X_{14}^{HBB}(t)\,dt\right] \Delta M_{dredge},$$
$$\Delta^{16}O = \left[(1 - f_{HBB})X_{16} + \frac{f_{HBB}}{t_{HBB}} \int_0^{t_{HBB}} X_{16}^{HBB}(t)\,dt\right] \Delta M_{dredge}, \quad (35)$$

where $t_{HBB}$ is the average time of exposure to the high temperatures at the base of the envelope. Details on how the time evolution of a species was calculated are given in Appendix A. The initial conditions to be used in the integrals in Eq. (35) are $X_{12}^{HBB}(t=0) = X_{12}$ and similar for oxygen, while $X_{13}^{HBB}(t=0) = X_{14}^{HBB}(t=0) = 0$.

If we also allow for a fraction ($f_{bur}$) of the envelope mass to be mixed downwards and processed by HBB (as defined above), the abundances of a general species $X$, after a dredge-up period and HBB during the interpulse period can be calculated from

$$X^{new} = \frac{X^{old} M_{env}(1 - f_{bur}) + \Delta X + \frac{f_{bur} M_{env}}{t_{HBB}} \int_0^{t_{HBB}} X(t)\,dt}{M_{env} + \Delta M_{dredge}}, \quad (36)$$

where $\Delta X$ is given by Eq. (35). The initial condition in the integral appearing in Eq. (36) is $X(t=0) = X^{old}$. The case of no HBB can be recovered using $f_{bur} = 0$ and $f_{HBB} = 0$.

### 2.10. *The numerical computations*

We have developed two very similar computer programs, one to calculate the evolution of a single star and another program which calculates the evolution of a sample of stars distributed according to a preset distribution function.

In the former program we first specify the initial mass and the metallicity of the star and the free parameters ($M_c^{min}$, $\eta_{EAGB}$, $\eta_{AGB}$,

$\lambda$ and whether or not HBB is included). The program then calculates the effects of the first dredge-up on the abundances and the mass lost up to the first TP. The core mass and luminosity at the first TP are calculated and for stars experiencing the second dredge up, the abundances after the second dredge-up are derived. Subsequently the program enters the AGB subroutine.

At each new time step, the updated luminosity is calculated and the "status" of the star is determined: carbon star ($C/O \geq 1.0$), S-star ($0.81 \leq C/O < 1.0$; Smith & Lambert 1986), M-star ($C/O < 0.81$), J-type or not ($^{12}C/^{13}C \lesssim 10$) and whether or not a certain mass loss rate, $\dot{M}_{IR}$, is exceeded (see Appendix C). The radius, mass loss rate and core growth rate are calculated. A new time step is determined from the condition that the core mass and the envelope mass may change by no more than a preset value (usually set at $0.001 M_{\odot}$), with the additional provisos that the luminosity peak and the luminosity dip are covered by at least one time step and that the timestep does not exceed the interpulse period. Having determined the time step, all masses (total, core, envelope, core growth since the last pulse) are updated. If the total time since the last TP is less than the interpulse period a new time step is calculated. If it exceeds the interpulse period, the abundances are updated and a new interpulse period is determined. Evolution ends when the envelope mass is decreased below $M_{end}$ or when the core mass exceeds the Chandrasekhar mass, so that the star ends as a supernova.

In the second code we calculate the evolution of a sample of AGB stars by selecting initial masses according to the probability that a star of initial mass $M$ is on the AGB. Stars which are presently on the AGB must have been born an appropriate time ago, so that the distribution function may be written as

$$N(M)\,\mathrm{d}M \propto \int_0^{t_{AGB}(M)} \mathrm{IMF}(M)\,\mathrm{SFR}(T_G - t_{pre}(M) - x)\,\mathrm{d}x,$$

where IMF (in $M_{\odot}{}^{-1}$) is the initial mass function ($\propto M^{-\alpha}$), SFR (in $M_{\odot}\,\mathrm{yr}^{-1}$) is the star formation rate, $t_{AGB}$ the lifetime of a star on the AGB, $T_G$ the age of the system and $t_{pre}$ the pre-AGB lifetime of a star.

Realising that $t_{AGB} \ll t_{pre}$ for all $M$ leads to

$$N(M)\mathrm{d}M \propto \mathrm{IMF}(M)\,\mathrm{SFR}(M)\,t_{AGB}(M), \quad M_{lower} < M < M_{upper}. \tag{37}$$

Estimates for $t_{AGB}$ are derived in Appendix B.

In the program initial masses are randomly selected according to the distribution function Eq. (37). From a relation between the initial mass and the pre-AGB lifetimes, the SFR and metallicity at the time of birth are deduced. The number of stars $N$ (usually 1000), $M_{lower}$, $M_{upper}$, the IMF, the SFR and the age–metallicity relation have to be specified. See Sect. 3 for details on the specific relations used for the LMC.

### *2.11. Limitations and uncertainties*

We attempted to bring together in this model all knowledge provided by presently available evolutionary calculations for AGB stars. However, the mere fact that these calculations do not reproduce all observational quantities (e.g. the luminosity function of carbon stars in the LMC) implies that evolution theory still needs improvement.

Also within the framework of the adopted approximations there are some limitations. For example, the dredge-up parameter, $\lambda$ [Eq. (34)], is assumed to be constant. In all likelihood it will depend, in a complex manner, on mass and composition. Secondly, a Reimers law was adopted to describe the mass loss rate on the AGB. Does this empirically derived law for red giants provide a good description of mass loss on the AGB? A third uncertainty lies in the initial abundances and the abundance changes prior to the AGB. Ideally one needs an age–metallicity relation for all important elements (He, C, N, O) separately. The few attempts to construct such relations for the Galaxy (Matteucci & François 1989, Rocca-Volmerange & Schaeffer 1990) give results which do not seem to agree with observations. For extragalactic systems age–metallicity relations for individual elements do not exist.

A fourth uncertainty lies in the fact that we only consider single star evolution. It has been established e.g. that almost all CH- and Ba II-stars and a significant fraction ($\sim 38\%$) of MS and S stars are binaries and that e.g. the R-stars show a normal binary frequency (McClure 1989; Smith & Lambert 1988; Brown et al. 1990). Iben & Tutukov (1989) estimate that $\sim 15$–$20\%$ of PN are expected to form in close binaries. Our calculations do not take into account close binary evolution and mergers.

## 3. The carbon star luminosity function in the LMC

Iben (1981) published an article entitled "The carbon star mystery: why do the low mass ones become such and where are the high mass ones gone?" In this article Iben compared the theoretically predicted LF of carbon stars and the observed LF of carbon stars in the LMC which at the time was determined rather accurately for the first time from deep surveys (Blanco et al. 1980). The difference was striking: the observed carbon stars in the LMC had bolometric magnitudes from $-3.5$ to $-6$ while the predicted range was $\sim -5$ to $-7.1$, the maximum luminosity at the tip of the AGB.

As indicated by the title of Iben's work, subsequent work has focussed on the formation of low-luminosity carbon stars and suggestions as how to solve the problem of the high luminosity carbon stars.

With regard to the formation of low luminosity carbon stars we refer to the reviews of Iben (1988) and Lattanzio (1989b). It seems that carbon recombination at low temperatures, semi-convection, convective overshooting and the mixing length parameter $\alpha$, play a role in the formation of low-luminosity carbon stars.

With regard to the high-luminosity carbon stars several explanations have been proposed (Iben 1981): A pause in the star formation and consequently an absence of young massive stars, hot bottom burning (HBB) which can prevent the formation of carbon stars because $^{12}C$ is transformed into $^{14}N$, a mass loss rate higher than the classical Reimers value or the formation of stars enshrouded in thick circumstellar envelopes. The last two arguments are of course closely related. Only detailed calculations can show if enhanced mass loss on the AGB produces stars with thick circumstellar shells, which could have escaped detection from optical surveys. Finally, Renzini et al. (1985) suggested that convective overshooting reduces $M_{up}$, the upper limit in initial mass of stars appearing on the AGB, from $\sim 8 M_{\odot}$ to $\sim 5 M_{\odot}$. The first argument, a pause in the star formation rate, has been dismissed by Iben (1981) and Reid et al. (1990), because there exist many Cepheids in the clouds which are the likely progenitors of the more massive AGB stars. The last argument, core overshooting, cannot be the sole solution to the problem

because even stars of $5M_{\odot}$ can reach high luminosities, as was noted by Reid et al. (1990). Hot bottom burning can prevent the formation of carbon stars (RV) but this implies that a star remains oxygen-rich for a longer time, thereby reaching higher luminosities. Although M-stars are known to exist with magnitudes in the interval $-6 \lesssim M_{\rm bol} \lesssim -7$ (Wood et al. 1983) there seems to be a general scarcity of high-luminosity AGB stars. This would exclude HBB as the solution to the absence of the high luminosity carbon stars and leaves an enhanced mass loss rate as the most important cause for the absence of high luminosity carbon stars.

In the models described below we have used the following parameters, appropriate for the LMC. The IMF-slope, SFR and age–metallicity relation were adopted from van den Hoek & de Jong (1991), see Fig. 4. These relations were derived by simultaneously modelling the current gas fraction, current metallicity and age–metallicity relation for the LMC, constrained by the best available ages and metallicities of LMC clusters. Assuming a power-law IMF (IMF$\propto M^{-\alpha}$) and a density dependent SFR, the age–metallicity relation for the LMC was best modelled with $\alpha = -2.72$. The age of the LMC is taken as 11 Gyr, about equal to the age of the Galactic disk (Rocca-Volmerange & Schaeffer 1990). The pre-AGB lifetimes of Iben & Laughlin (1989) are used to relate the initial mass to the pre-AGB lifetimes.[1] From this relation it is also derived that stars down to $M_{\rm lower} = 0.93M_{\odot}$ have lived long enough to have reached the AGB. If the mass loss rate on the RGB (and possibly the E-AGB) is high enough though, the stars with the lowest initial masses will not reach the AGB but will turn into white dwarfs on or after the RGB. From BI1 we derive $M_{\rm upper} = 8.2M_{\odot}$ for typical LMC abundances. For the Chandrasekhar mass we assume $M_{\rm Ch} = 1.2M_{\odot}$ (Hamada & Salpeter 1961).

To compare the model results to the observations we have combined the observed LMC carbon star LF of Cohen et al. (1981) with the data presented by Richer et al. (1979).

Blanco et al. (1980) surveyed three 0.12 deg$^2$ fields in the LMC, complete down to $M_{\rm bol} \approx -2$. They found 186 carbon stars. Cohen et al. derived bolometric magnitudes for 165 of them. One carbon star brighter than $M_{\rm bol} = -5.8$ was discovered. Westerlund et al. (1978), surveying 62.5 deg$^2$ down to $M_{\rm bol} \approx -4.5$, discovered 302 carbon stars. Richer et al. presented $R, I$ photometry for 112 of them. We transformed these into bolometric magnitudes using the bolometric corrections of Cohen et al. In this sample, 28 have $M_{\rm bol} < -5.8$.

Richer et al. (1979) and Richer (1981a) have investigated the relative importance of the J-type carbon stars, carbon stars enriched in $^{13}$C, in both surveys. Richer found 3 J-type stars among the 23 he investigated in one of the Blanco et al. fields which contained a total of 70 carbon stars and Richer et al. found 7 among the 40 stars they investigated of the Westerlund et al. survey.

In Fig. 5 the observed LF of carbon stars in the LMC is presented, scaled to a distance modulus of the LMC of 18.5 [see Table 6 of Jacoby et al. (1990) for a compilation of distance determinations to the LMC. A recent determination with the HST for SN 1987A gave $18.50 \pm 0.13$ (Panagia et al. 1991)]. The solid line is the total LF, while the dotted line is the contribution of the J-type carbon stars, blown up by a factor of 5. The observed number of J-type stars in each bin was scaled using the respective discovery rate in both fields and then the LF of both fields were weighted with the total discovery rate of carbon stars in the Blanco et al. and Westerlund et al. surveys. The LF of the J-type stars is uncertain due to the small numbers involved.

From Fig. 5 it is derived that carbon stars exist up to $M_{\rm bol} \approx -6.5$ but that they are rare. Approximately 1% is brighter than $M_{\rm bol} = -5.8$. The peak of the LF is at $M_{\rm bol} = -4.875$ (center of bin). The distribution of the J-type stars is bimodal. There is a small fraction ($\sim 0.1\%$) of high luminosity J-type carbon stars,

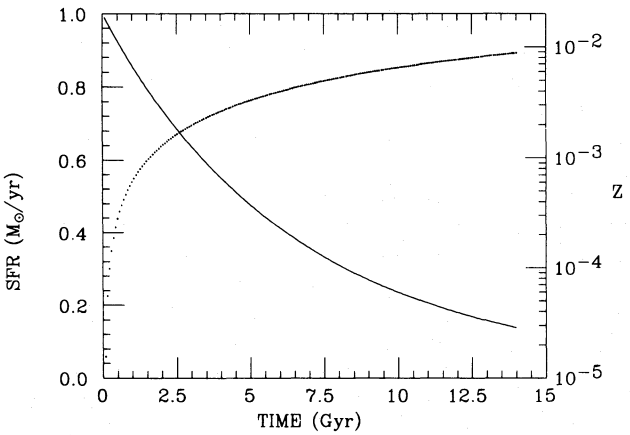


**Fig. 4.** The age–metallicity relation (dotted curve, righthand scale) and star formation rate (solid curve, lefthand scale) in the LMC adopted from van den Hoek & de Jong (1992)

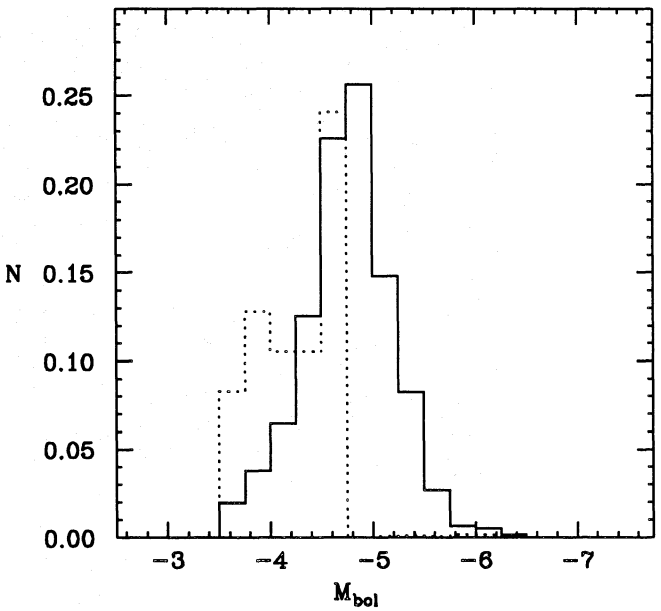


**Fig. 5.** The observed luminosity function (LF) of carbon stars in the LMC for a distance modulus of 18.5. The solid line is the total LF, while the dotted line is the LF of the J-type carbon stars, multiplied by a factor of 5. The total LF is normalised to unity

[1] In fact Iben & Laughlin presented á fit to the lifetimes needed to reach the white dwarf (WD) stage. Because the main sequence and RGB lifetimes dominate all other evolutionary phases, this is essentially equal to the pre-AGB lifetime.

possibly connected to HBB and a more significant fraction ($\sim 10\%$) of low–luminosity J-type carbon stars. They dominate the lowest luminosity bins. The non-J-type carbon stars in the LMC are important for $M_{\rm bol} < -4$. The origin of the low–luminosity J-type carbon stars is less clear. These stars might be descendents of, or related to, the R-type stars, which are observed in the Galactic bulge up to $M_{\rm bol} \approx -2.8$ (Westerlund et al. 1991b).

To allow for an observational error in the observed LF as well as for the depth of the LMC ($1\sigma = 0.04$ mag as quoted in Jacoby et al. 1990) and the intrinsic variability of stars on the AGB, all the theoretical calculated LFs shown below are convolved with a Gaussian of width $1\sigma = 0.20$ mag.

Besides the observed carbon star LF, the observed ratio of carbon-to-oxygen rich stars (C/M-ratio) in the LMC will be used as an additional constraint to the model.

For the carbon-to-oxygen rich star ratio a value of C/M $\approx 2$ is often quoted but some care should be taken since this ratio strongly depends on spectral type of the M stars that are taken into account. Blanco & McCarthy (1983) give C/M2+ = $0.2 \pm 0.1$, C/M5+ = $0.80 \pm 0.03$, C/M6+ = $2.2 \pm 0.1$ respectively. The question is therefore: what is the range in spectral type of oxygen-rich TP-AGB stars, and what is the contamination of e.g. E-AGB stars for a given spectral type?

Hughes (1989) and Hughes & Wood (1990) have made a survey for LPV in the LMC and determined spectral types for many of them. The stars they found have luminosities which indicate that they are on the AGB, but it is not possible to discriminate conclusively between the E-AGB and the TP-AGB phase. In any case, they find that most LPV have spectral types M 5 or later and that C/M = 0.63. It seems plausible that most stars in the LMC with spectral type M 5 and later are on the TP-AGB. Based on the previous estimates we will assume a theoretically predicted C/M ratio of thermal pulsing AGB stars in the LMC of $0.6 < {\rm C/M} < 2.5$ as in agreement with observations.

### *3.1. The low–luminosity tail of the LF of carbon stars in the LMC*

In this section the parameters which influence the low–luminosity tail of the carbon star LF will be discussed.

The standard model has the following parameters: pre-AGB mass loss rates of $\eta_{\rm RGB} = 0.86$ and $\eta_{\rm EAGB} = 3.0$, mass loss rate on

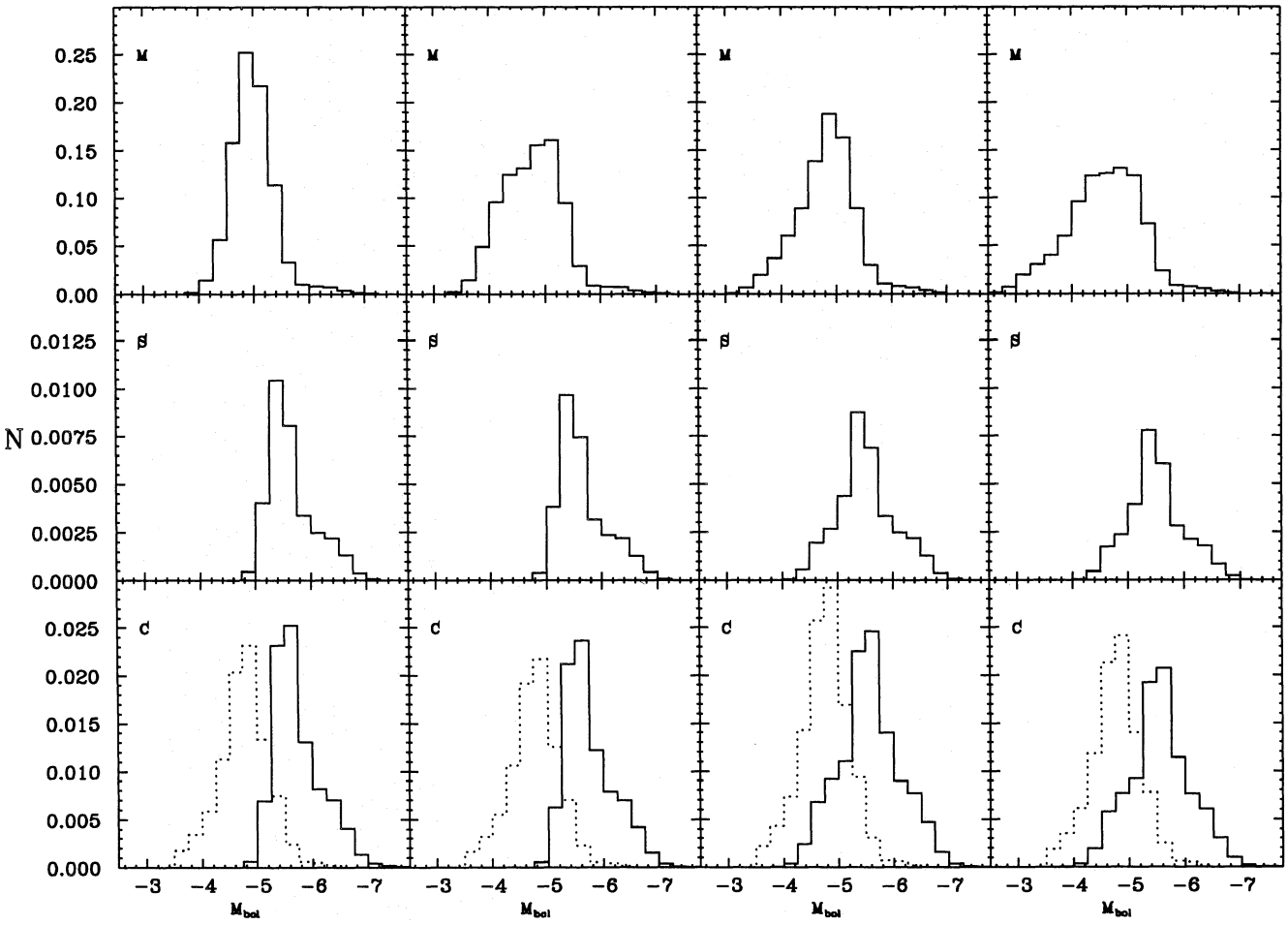


**Fig. 6.** The importance of the variation in luminosity during the flashcycle and the first few pulses on the luminosity function. From left to right the models (N, N), (N, Y), (Y, N) and (Y, Y) where the first letter indicates whether the variation in luminosity during the flashcycles was included and the second one if the effect of the first few pulses was included. For each model the top figure indicates the oxygen-rich stars, the middle one the S-stars and the bottom figure the carbon stars. The LF is plotted in such a way that the sum over all bins (M + S + C) gives unity. The dotted line represents the observed carbon star LF of Fig. 5

the AGB $\eta_{AGB}=3.0$, minimum core mass for dredge-up according to Eq. (32), dredge-up parameter $\lambda=1/3$, no convective overshooting, no HBB.

The fact that the luminosity during the first few pulses is below the core–mass–luminosity relation, and the fact that the luminosity is not constant during the flashcycle were long known, but never simultaneously included in any synthetic evolution model before. Iben (1981) approximately included the effects of the flashcycle in his calculations and Bedijn (1988) the effect of the first few pulses. The importance of taking both these effects into account is demonstrated in Fig. 6 where we plotted the LF of M, S and C stars for the standard model for the following parameters (from left to right): not taking into account the variation during the flashcycle (no "flashcycle") and the effect of the first few pulses (no "first few pulses"), no "flashcycle" but "first few pulses" included, "flashcycle" included but not the "first few pulses", both "flashcycle" and "first few pulses" included.

The carbon star LF when neither the flashcycle and the effect of the first few pulses is included outlines the "carbon star mystery" of about 10 years ago. Compared to the observed LF in Fig. 5 there are no low–luminosity carbon stars and too many bright ones.

For the standard model, taking into account the effect of the "first few pulses" has only effect on the M-star LF. The LF extends about 0.5 mag to lower luminosities. This is indeed expected based on Fig. 2. The fact that the carbon star LF remains unchanged is simply because stars become carbon stars after the sixth TP, which is the timescale adopted to go from the first TP to full amplitude pulses. The largest effect of the flashcycle is to lower the low–luminosity tail of the LF by about 0.8 mag. This is expected based on the assumed properties of the flashcycle (Table 4).

It is obvious from comparing the left and rightmost LF in Fig. 6 that the effects of the flashcycle and the first few pulses are rather large and should not be neglected. It is also obvious by comparing the rightmost carbon star LF of Fig. 6 with the observed LF that these two effects alone are not sufficient to bring the observed LF in accord with the predicted one. The standard model including the "flashcycle" and the "first few pulses" still predicts too few low luminosity carbon stars and too many bright ones.

One could assume an even larger effect of the luminosity dip (one would need $\Delta\log L_{dip}\approx -0.7$) but unless the evolutionary models are completely wrong, this seems not a viable option. Besides, this does not solve the discrepancy of the high–luminosity carbon stars and the wrong luminosity of the peak of the distribution. A more promising solution to the discrepancy at the low–luminosity end of the C-star LF is that the minimum core mass for dredge-up, $M_c^{min}$, is too high in the standard model. An alternative solution, which will be investigated later, is that the amount of carbon dredged up at a TP is too low. In evolutionary calculations $M_c^{min}$ is determined by the adopted mixing length parameter, which is very uncertain. BS4 showed that by (suddenly) increasing $\alpha$ to 3 they could produce a carbon star with a core mass of 0.566 from a star of initial mass $1.2M_\odot$. Dredge-up started immediately at a core mass of 0.566, far below the value in the standard model of $M_c^{min}\approx 0.66$ [Eq. (32) with $Y=0.25$, appropriate for the LMC].

In Fig. 7 the carbon star LF is plotted (normalised to 1 in each panel) for the standard model but with $M_c^{min}=0.66$, 0.64, 0.62, 0.60, 0.58 and 0.56. Decreasing the minimum core mass for dredge-up shifts the peak of the carbon star LF to lower values but this effect is small, about 0.5 mag. Decreasing $M_c^{min}$ is not sufficient to let the predicted and observed LF agree. Because the observed LF starts at $M_{bol}\approx -3.5$ we can conclude that $M_c^{min}\geq 0.58$. Lowering the minimum value for dredge-up results in a longer carbon star phase. For the six values of $M_c^{min}$ reported above the C/M ratio increases from 0.11, 0.15, 0.25, 0.38, 0.59 to 0.74. The ratio of S-stars to carbon stars is almost constant: S/C = 0.31, 0.30, 0.29, 0.28, 0.27, 0.26.

Although we have established that the onset of the carbon star LF can be well explained with $M_c^{min}\approx 0.58$, the peak of the

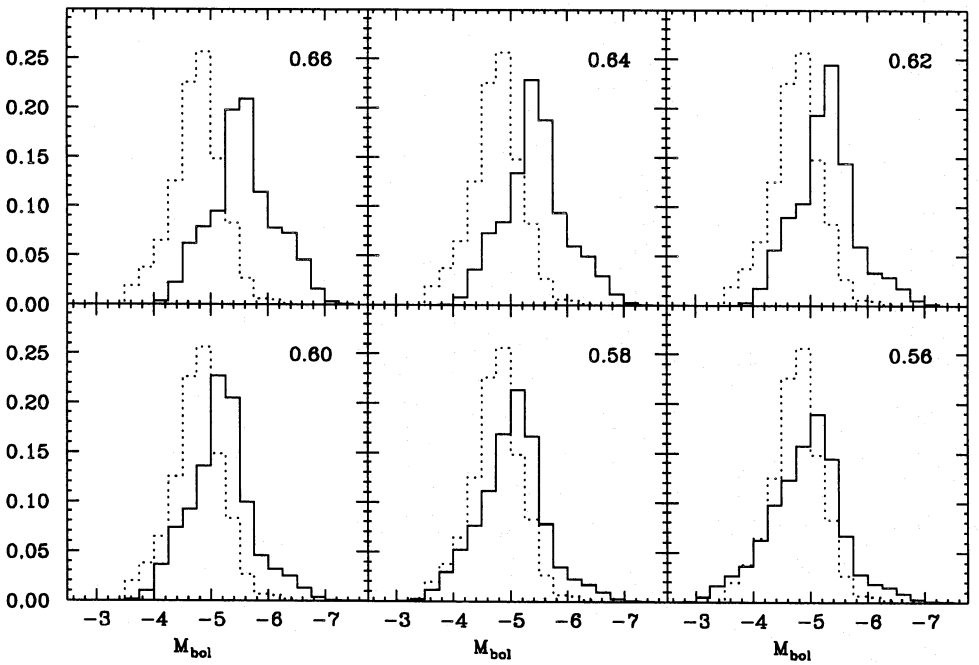


**Fig. 7.** The influence of lowering the minimum mass for dredge-up on the carbon star LF. The LF is normalised to unity. The values of $M_c^{min}$ (in $M_\odot$) are indicated in each panel. The value of C/M increases from 0.43 to 1.8 and the peak is shifted by 0.5 mag to lower luminosities. The dotted line represents the observed carbon star LF of Fig. 5

predicted LF is still at a luminosity which is too high. To steepen the carbon star LF we consider three possibilities: (1) a change in the distribution of stars on the AGB; (2) a decrease in the envelope mass of low-mass stars before the first TP and (3) an increase in the amount of carbon dredged up after each TP. The results are gathered in Fig. 8 and compared to the standard model with $M_c^{min}=0.58$ (panel a).

Since the initial mass function is the dominant factor determining the distribution of stars on the AGB the slope of the IMF was changed from $-2.72$ to $-3.5$. This results in a relative increase of low-mass stars which should become carbon stars at lower luminosities. This is indeed found (panel b) but the change in the LF is small.

Decreasing the envelope mass of the low-mass stars before the first TP, i.e. increasing $\eta_{RGB}$, has two opposite effects. There is less oxygen in the envelope so the star should become a carbon star at lower luminosities. On the other hand the lifetime is reduced, so the star experiences less thermal pulses resulting in less dredge up of carbon. From panel (c) we deduce that the latter effect wins. There is a small shift to higher luminosities.

The amount of carbon dredged up after each TP is determined by $\lambda$, the total amount of matter dredged up relative to the amount of matter processed between two successive thermal pulses and $X_{12}$, the abundance of carbon in the material that is dredged up. In the standard model 7.3% of all processed material is carbon ($\lambda=1/3$, $X_{12}=0.22$). In panel (d) this is increased to 16.5% ($\lambda=0.75$, $X_{12}=0.22$). The agreement with the observed LF is very good. The peak of the LF is now at the correct luminosity. The C/M-ratio is 1.4 in this model which is in good agreement with observations.

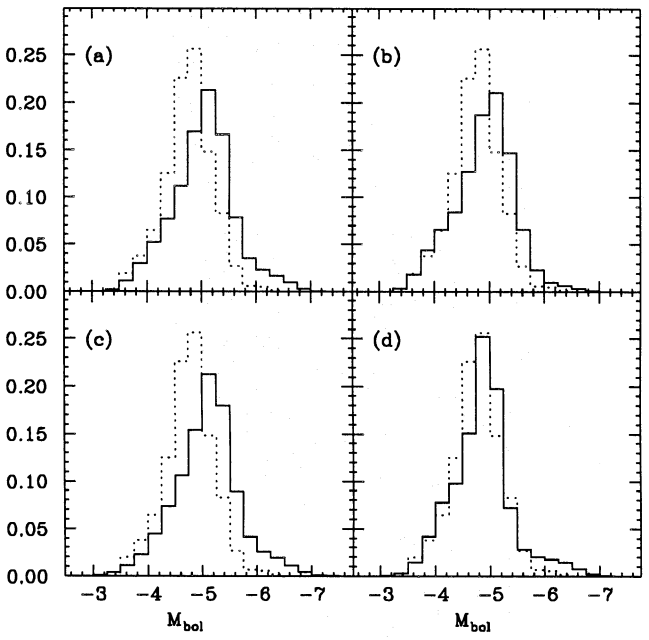


**Fig. 8.** The normalised carbon star LF for the following models: (a) standard model with $M_c^{min}=0.58M_\odot$ ($\alpha=-2.72$, $\eta_{RGB}=0.86$, $\lambda=1/3$); (b) the slope of the IMF changed to $\alpha=-3.5$; (c) pre-AGB mass loss rate for the low-mass stars increased to $\eta_{RGB}=2.5$; (d) the amount of carbon dredged-up at each TP increased from 7.3% to 16.5%. Only an increase in the amount of carbon dredged up at each TP is capable of bringing the observed and predicted carbon star LF in agreement. The dotted line represents the observed carbon star LF of Fig. 5

Although a distance modulus of 18.5 seems to be the most reliable one, we have considered distance moduli of 18.25 and 18.75. The latter value is incompatible with the observed carbon star LF since it is not possible to shift the LF to much lower luminosities than what is achieved with the $M_c^{min}=0.58$, $\lambda=0.75$ model. For a distance modulus of 18.25 we performed a similar analysis as described above. We find that a model with $M_c^{min}=0.60$ and $\lambda=0.6$ (i.e. 13% carbon dredged up after each TP) predicts a carbon star LF which is in agreement with the observed one if shifted to a distance modulus of 18.25. The C/M-ratio in this model is 0.69 which is still in agreement with observations.

We conclude that the low–luminosity tail and the peak of the carbon stars LF can be explained equally well by two models. If the LMC has a distance modulus of 18.25, a model with a minimum core mass for dredge-up of $M_c^{min}=0.60$ and with 13% of the processed material in carbon fits the observed carbon star LF well. For the commonly accepted distance modulus of 18.5 the numbers of the best model are $M_c^{min}=0.58$ and 16.5%. We did not consider distance moduli less then 18.25 because they are unrealistically low. Distance moduli of $\gtrsim 18.6$ are excluded by our model. Only when the core masses at the first TP for the low-mass stars are lower than assumed in this model it *might* be possible to obtain a good fit for larger distance moduli.

The values of $M_c^{min}$ found to be in agreement with observations are lower than found in existing models (except the one ad hoc model of BS4). Lattanzio (1989a) found values of $M_c^{min}$ of 0.605 for a $Z=0.001$, $M=1.5M_\odot$ model and $M_c^{min}=0.63$ in a $Z=0.001$, $M=1M_\odot$ and a $Z=0.01$, $M=1.5M_\odot$ model.

### *3.2. The high–luminosity tail of the LF of carbon stars in the LMC*

As briefly pointed out earlier the high–luminosity tail of the carbon star LF could, in principle, depend on four factors: the mass loss rate, incompleteness of the optical surveys, HBB and/or convective overshooting. They will be discussed in that order.

We first consider the combination of the mass loss rate and optical obscuration. In Appendix C we derive that a maximum of 3% of all carbon stars brighter than $M_{bol}=-6$ could have been missed by the optical surveys. Based on radiative transfer calculations we derive in Appendix C the critical mass loss rate $\dot{M}_{IR}$ at which a carbon star in the LMC becomes invisible. The value of $\dot{M}_{IR}$ scales with the factor $F_{IR}$ which depends on the assumed dust properties and the dust-to-gas ratio. It is estimated in Appendix C that $F_{IR}$ is in the range 0.04–100. In the calculations presented below $F_{IR}$ was varied in such a way that 3% of all carbon stars brighter than $M_{bol}=-6$ were obscured. The model then predicts the degree of obscuration at other luminosities. In Fig. 9 the optical carbon star LF is presented for $\eta_{AGB}=\eta_{EAGB}=3, 5, 8$. The scale factor $F_{IR}$ was found to be 10, 14, 22 respectively. The overall C/M ratio is 1.44, 0.88 and 0.45. Of all carbon stars 3.8, 1.8 and 0.7% are brighter than $M_{bol}=-6$. The observed fraction is 1.3%. The overall fraction of obscured carbon stars is 0.12, 0.07 and 0.03%. For the M and S stars the obscured fraction is even less.

We conclude that obscuration is not important. Even when the optical surveys have missed 3% of carbon stars brighter than $M_{bol}=-6$ (which is in fact an upperlimit) the overall degree of obscuration is $\sim 0.1\%$ which is negligible. Since the mass loss rate of a star scales with $L$ in Reimers law but the critical mass

loss rate at which obscuration occurs, approximately with $L^{0.5}$ this is not surprising.

A second conclusion, based on the overall shape of the LF (too many carbon stars at mid– and low–luminosities), the C/M ratio and the fraction of carbon stars brighter than $M_{\rm bol}=-6$ is that $\eta_{\rm AGB}<8$. The model with $\eta_{\rm AGB}=5$ fits the observations quite well.

We will now consider the influence of HBB. Hot bottom burning slows down, or even prevents the formation of carbon stars by burning newly dredged-up matter into $^{14}$N during the interpulse period. RV have extensively modelled HBB and we included in a simple way these effects for their $\alpha=2$ case, which gives the most HBB. Details are given in Sect. 2.9.4 and Appendix A. For the $\alpha=2$ case, HBB is important for stars with $M_{\rm initial}\gtrsim 3.3 M_{\odot}$, so it is expected that HBB can in principle influence the high–luminosity tail of the carbon star LF.

In Fig. 10 we present the M, S and C star LF for three models: (1) the standard model without HBB and with $\eta_{\rm AGB}=\eta_{\rm EAGB}=3$, (2) the same model with HBB and (3) a model with HBB and $\eta_{\rm AGB}=\eta_{\rm EAGB}=5$. The effect of obscuration is included. The LF of stars with $^{12}C/^{13}C<10$, multiplied by 5, is given by the dotted lines. The C/M ratio is 1.44, 1.28 and 0.85 respectively. The fraction of carbon stars brighter than $M_{\rm bol}=-6$ is 3.8, 1.2 and 0.7%. The fraction of J-type carbon stars brighter than

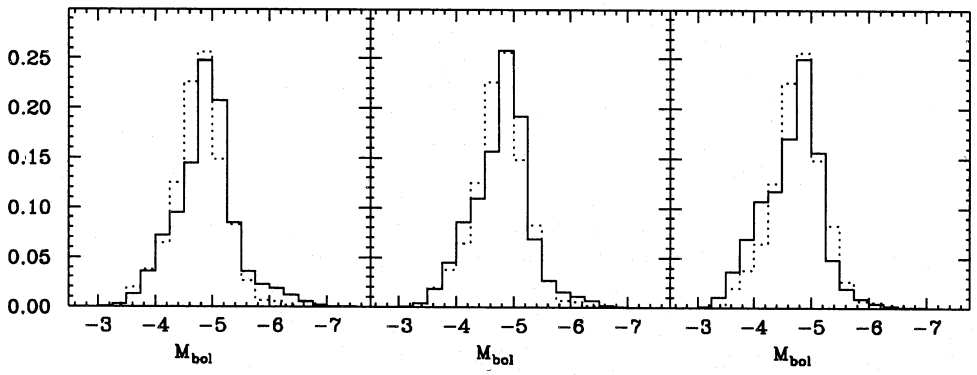


**Fig. 9.** The effect of mass loss and obscuration on the optical carbon stars LF. From left to right models with $\eta_{\rm AGB}=\eta_{\rm EAGB}=3$, 5, 8 respectively. The $\eta_{\rm AGB}=8$ model predicts too few high–luminosity and too many low–luminosity carbon stars. The dotted line represents the observed carbon star LF of Fig. 5

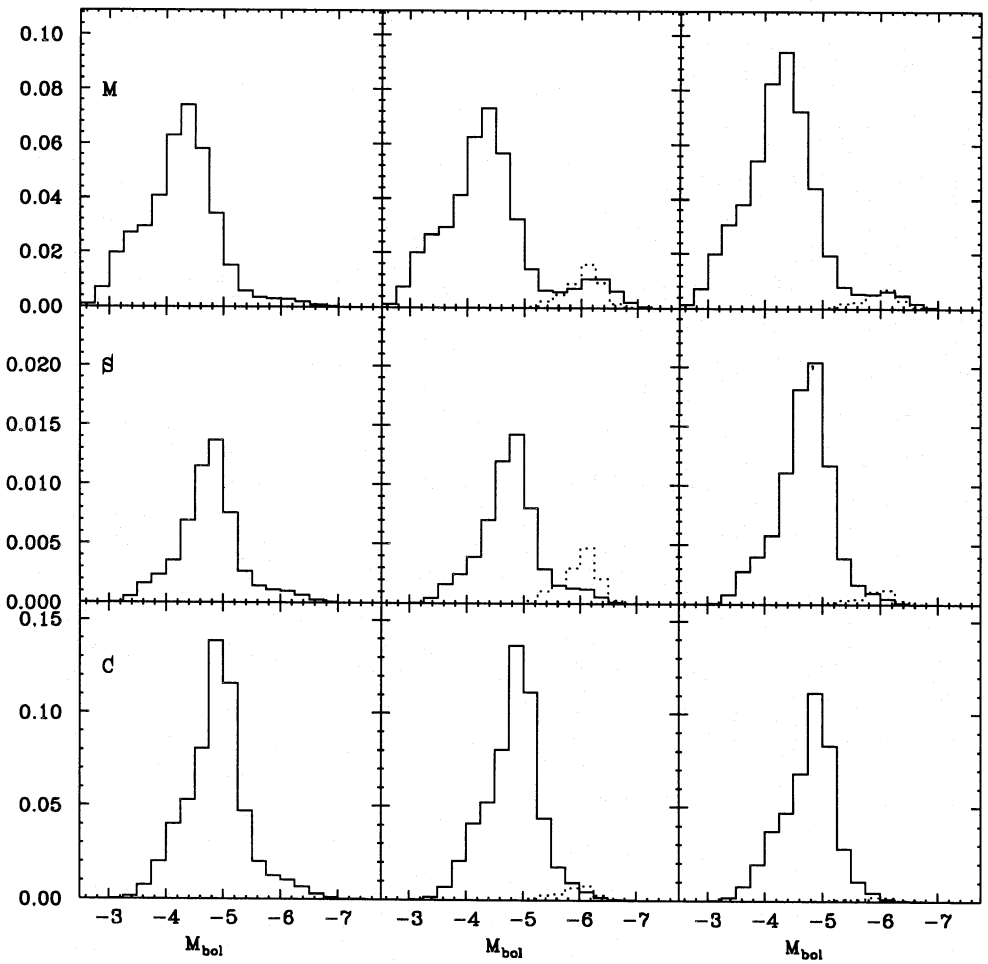


**Fig. 10.** The effect of HBB. The luminosity functions (LF) of M, S and C-stars (top to bottom) are plotted for the following models (from left to right): no HBB, $\eta_{\rm AGB}=\eta_{\rm EAGB}=3$; HBB, $\eta_{\rm AGB}=\eta_{\rm EAGB}=3$; HBB, $\eta_{\rm AGB}=\eta_{\rm EAGB}=5$. The LF of stars with $^{12}C/^{13}C<10$, multiplied by 5, is indicated by the dotted lines. One sees how the luminous carbon stars are transformed into ($^{13}$C-rich) M-stars when HBB is included

$M_{bol} = -5$ is 0, 2.6 and 1.2% and 0, 0.9 and 0.4% overall. The observed number of high–luminosity J-type carbon stars is 0.5% below $M_{bol} = -5$ and ~0.1% overall.

Given the uncertainty in the J-type carbon star LF due to the small numbers involved, we conclude that our model for HBB in combination with $\eta_{AGB} = \eta_{EAGB} = 5$ can account for the overall shape of the high–luminosity tail as well as roughly for the observed number of high–luminosity J-type stars. Our model predicts that there also should be M and S stars which have $^{12}C/^{13}C < 10$. Roughly 0.8% of the M-stars and 1% of the S stars are predicted to be enriched in $^{13}C$ in the $\eta_{AGB} = \eta_{EAGB} = 5$ model. This prediction will be difficult to verify because these stars are probably too faint to obtain the very high resolution spectra necessary to observe the $^{13}CO$ bands in the near infrared. The very luminous MS-stars (Wood et al. 1983; Lundgren 1988) should be considered first rate candidates for such an analysis when improved observational techniques allow this.

Finally, we briefly discuss the effect of convective overshooting. The effect of convective overshooting is rather difficult estimate in our models, because the formulae presented in Sect. 2 have been derived from classical models without convective overshooting. Because little or no evolutionary calculations have been performed for AGB stars with convective overshooting models we have restricted ourselves to a zeroth order approximation of convective overshooting, based upon the fact that convective overshooting effectively increases the core mass of a star in such a way that a star of initial mass $M$ behaves like a star of mass $f_{os} M$ ($f_{os} > 1$, "os" stands for overshooting) without convective overshooting. The factor $f_{os}$ was determined by comparing the MS lifetimes and the mass for which the HeCF occurs from evolutionary calculations with and without convective overshooting. A factor $f_{os} \approx 1.2$–$1.4$ is appropriate for models with small convective overshooting ($d = 0.25 H_p$; Maeder & Meynet 1989), while for models with strong convective overshooting ($d = 1 H_p$; e.g. Chiosi et al. 1987) $f_{os} \approx 1.3$–$1.6$ seems appropriate. Convective overshooting is only important for stars with $M_{initial} \gtrsim 1.2 M_\odot$, so $f_{os}$ always equals 1 for stars below this limit. Selecting star from interval $M_{lower} \leq M \leq (M_{upper}/f_{os})$ we calculated the evolution as if the core mass was for a star of mass $f_{os} M$. The main changes relative to the non-convective overshooting models are threefold. Firstly, substantial mass loss on the RGB is restricted to stars with $M \lesssim 1.6 M_\odot$, because stars above this limit will not experience the HeCF. Secondly, for a given initial mass the core mass at the first TP will be larger and thirdly, the envelope mass will be smaller.

A comparison of models ($M_c^{min} = 0.58 M_\odot$, $\lambda = 0.75$, $\eta_{AGB} = \eta_{EAGB} = 5$, HBB included) calculated with and without convective overshooting (using $f_{os} = 1.2$) shows that the differences are small. The C/M ratio e.g. is reduced from 0.85 to 0.73. The shape of the carbon star LF remains virtually unchanged. The largest difference is in the initial–final mass relation. Because a star of mass $M$ is supposed to evolve like a star of mass $f_{os} M$ without overshooting, the final mass of a star will be higher than the final mass of the same star without overshooting. Stothers (1991) showed that all tests for the presence of convective overshooting are consistent with $d/H_p = 0$, and that the best tests place an upperlimit of $d/H_p < 0.2$. Convective overshooting will not affect the conclusions of this paper.

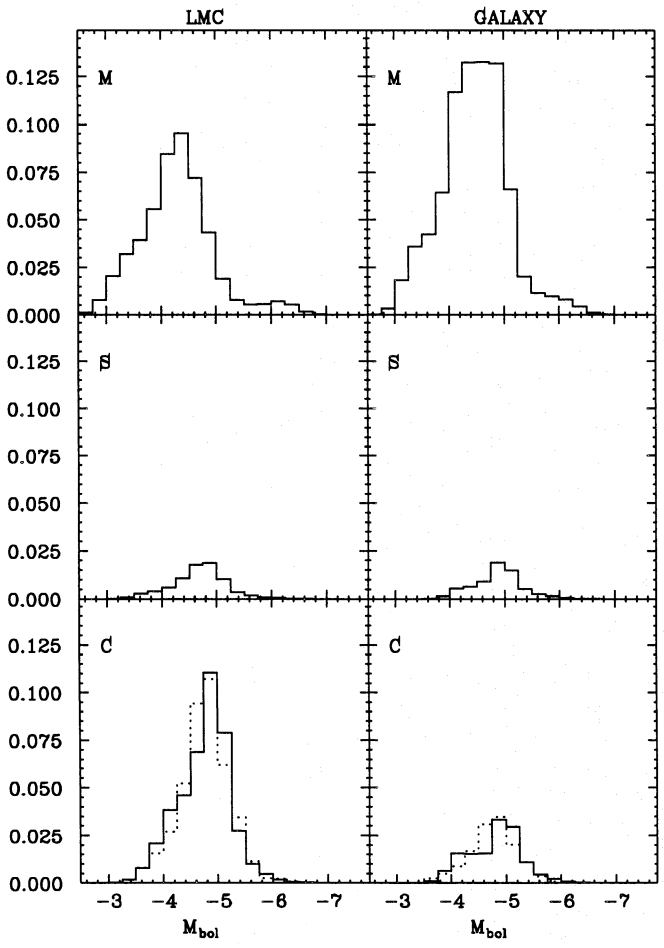


**Fig. 11.** The LF of M, S and C-stars for the final LMC model with parameters $M_c^{min} = 0.58 M_\odot$, $\lambda = 0.75$, $\eta_{AGB} = \eta_{EAGB} = 5$, HBB included. For the same set of parameters a Galactic model was calculated using the appropriate SFR, IMF and age–metallicity relation of van den Hoek & de Jong (1992). The dotted curve is the observed LMC carbon star LF of Fig. 5

## 4. Discussion and conclusions

In Fig. 11 the M, S and C-star LF is plotted for the best model of the LMC. The parameters are $M_c^{min} = 0.58 M_\odot$, $\lambda = 0.75$, $\eta_{AGB} = \eta_{EAGB} = 5$, $\eta_{RGB}$ 0.86, HBB included. We find that M, S and C stars occur in the ratio 0.501 : 0.077 : 0.422. The predicted (solid) and observed (dotted) carbon star LF agree very well. The predicted C/M ratio (0.85) lies within the observed range (0.6–2.5).

The chemical nature of AGB stars is based upon the C/O abundance ratio. We have assumed that the transition from M to S star occurs at C/O = 0.81 and from S to C star at C/O = 1.0. In particular the former value is uncertain. To illustrate this uncertainty we recalculated the LF for the final LMC model assuming that the M to S star transition occurs at C/O = 0.90. We find slightly different ratios of M, S and C stars, 0.539 : 0.039 : 0.422. The LF are virtually unchanged. The C/M ratio drops to 0.78, while the S/C ratio drops from 0.18 to 0.093. We conclude that the average lifetime of the S star phase approximately scales like $\sim(1-\delta)$, where $\delta$ is the assumed C/O ratio of the M to S transition.

We cannot distinguish between models with a high $\lambda$ and a standard value of the carbon abundance after a TP ($X_{12}=0.22$) or vice versa. All models with $\lambda X_{12}=0.165$ fit the observations. Although a model with a higher $X_{12}$ results in less helium being dredged up, and a model with higher $\lambda$ results in lower final masses, these effects are too small to be used to determine if $\lambda$ or $X_{12}$ are different from the standard values ($\lambda=1/3$, $X_{12}=0.22$; $\lambda X_{12}=0.073$).

The minimum core mass for dredge-up is lower and the dredge-up efficiency is higher than found in published evolutionary calculations ($M_c^{\rm min}\gtrsim 0.60M_\odot$, $\lambda\approx 1/3$). However these models do not predict carbon stars at the observed low–luminosities. Only the model of BS4, when they arbitrarily increased the mixing-length parameter from 1 to 3, predicts the low–luminosity carbon stars observed. Recently, Sackmann et al. (1990) and Sackmann & Boothroyd (1991) showed that with their code and for certain opacities (LAOL including molecular opacities) a mixing-length of $\alpha=2.1$ was required to obtain a standard solar model and to explain the observed position of the red giant branch. The value they used in their earlier AGB calculations was $\alpha=1.0$. Because an increase in the mixing-length parameter reduces the luminosity at which dredge-up begins, it is not surprising that the old BS models did not predict carbon stars at the observed low luminosities. We suggest that a systematic underestimate of the mixing-length parameter is the reason that evolutionary calculations could not produce carbon stars at the observed low–luminosities.

Taking the SFR, IMF ($\alpha=-2.55$) and age–metallicity relation for the solar neighbourhood from a recent model (van den Hoek & de Jong 1992) and assuming that the AGB evolution parameters adopted for our final LMC model hold for the solar neighbourhood, the LF in Fig. 11 was calculated for the Galaxy. The shape of the carbon star LF is only slightly different from that in the LMC. This supports the assumption usually made by e.g. Groenewegen et al. (1992) that the mean luminosity of Galactic carbon stars is about equal to LMC carbon stars. Compared to the LMC the C/M ratio is reduced from 0.85 to 0.17. The observed value for the C/M ratio in the solar neighbourhood is $\sim$0.01 (Blanco & McCarthy 1981) which suggests that either $M_c^{\rm min}$ is higher, $\lambda$ lower or $\eta_{\rm AGB}$ higher in the Galaxy than in the LMC. The peak of the oxygen-rich AGB stars is increased from $\sim 4400L_\odot$ in the LMC to $\sim 5500L_\odot$ in the Galaxy. In Fig. 12 the initial–final mass relation is presented for the LMC (crosses) and the Galactic model (circles) and compared to the observations. The observational data was taken from Weidemann & Koester (1983) and references therein and supplemented with new results from Koester & Weidemann (1985) and Reimers & Koester (1988, 1989). Instead of plotting individual points with their errors the two solid lines in Fig. 12 give the maximum and minimum final mass allowed for by the data for a given initial mass. In general there is good agreement for the low mass stars. For the Galactic model the final masses for the massive stars are in agreement with the observations. The discrepancy for the LMC model is probably not significant since the observations refer to WD in the solar neighbourhood and therefore should be compared to the solar neighbourhood model.

With our mass loss rates the difference between final core mass and core mass at the first TP is $\lesssim 0.03M_\odot$ (see Table 5). This means that the initial–final mass relation strongly reflects the initial-core mass at the first TP-relation [Eqs. (1) and (4)] which changes in slope near $3M_\odot$ (see Fig. 1). Figure 12 shows that it is difficult to obtain good agreement for the high mass stars. This is probably due to the fact that our algorithms for high mass stars are fitted to evolutionary calculations which neglected mass loss. This probably resulted in an overestimate of the core mass at the first TP.

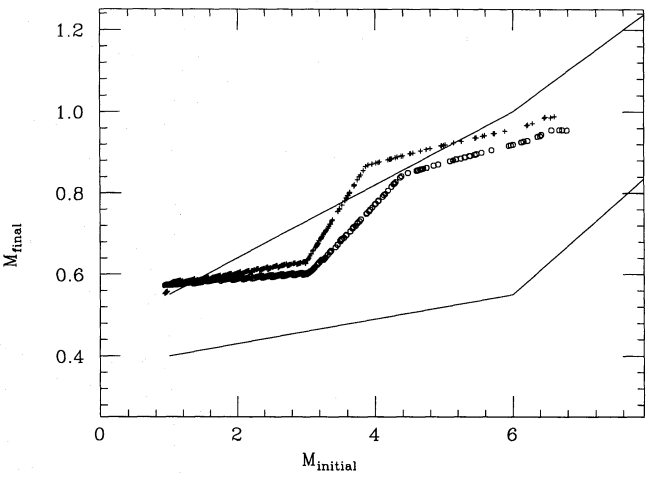


**Fig. 12.** The initial–final mass relation for the LMC (crosses) and Galactic model (circles). The two solid lines indicate the minimum and maximum final mass allowed for by the observations of white dwarfs in the solar neighbourhood.

We calculated the average final mass of the stars at the end of the AGB for the best model for the LMC and compared this to the average mass of the central stars of planetary nebulae. The mean value ($M_f=0.62M_\odot$) agrees well with the observed value of $0.60\pm 0.02M_\odot$ (Barlow 1989; Dopita & Meatheringham 1990, 1991; Clegg 1991). No selection effects are included in the theoretically predicted distribution. For example, the probability of observing a PN on the horizontal evolution track through the HR diagram is much higher for a low mass PN. On the other hand, some post-AGB objects of very low core mass ($M_c\lesssim 0.56M_\odot$) may evolve so slowly that they never become a PN, or are not recognised as such. This depends on the uncertain post-AGB mass loss rate, which determines the crossing time through the HR diagram.

We have so far concentrated on the global evolution of a distribution of AGB stars. For some combination of input parameters we have calculated the AGB evolution for selected initial masses. Some relevant quantities are collected in Table 5. We have considered the final model for the LMC ($\eta_{\rm RGB}=0.86$, $\eta_{\rm AGB}=\eta_{\rm EAGB}=5$, $M_c^{\rm min}=0.58$, $\lambda=0.75$, including HBB), labelled model 1, a model identical to model 1 but with $M_c^{\rm min}=0.59$, $\lambda=0.7$ (model 2), a model identical to model 1 but with $Z=0.02$ (model 3) and a model identical to model 3 but with $\eta_{\rm AGB}=\eta_{\rm EAGB}=7$ (model 4). In Table 5 the lifetime of the M, S and C phases are listed together with the total AGB lifetime, the pulse number at which the star became a carbon star, the total number of pulses on the AGB, the final mass and the core mass growth on the AGB [$=M_f-M_c(1)$], the total mass lost on the AGB and the average mass loss rate on the AGB. We conclude that mass loss dominates core growth by one to two orders of magnitude and that the average mass loss rate on the AGB increases from $10^{-6}\,M_\odot\,{\rm yr}^{-1}$ for the low mass stars to well over $10^{-5}\,M_\odot\,{\rm yr}^{-1}$ for the most massive stars.

**Table 5.** Results for some models

| $M$ | Model | $Z$ | $T_M$ | $T_S$ | $T_C$ | $T_{AGB}$ | $N_C$ | $N$ | $M_F$ | $\Delta M_c$ | $\Delta M_{AGB}$ | $\dot{M}_{AGB}$ |
|---|---|---|---|---|---|---|---|---|---|---|---|---|
| 0.93 | 1 | 0.0020 | 231 | — | — | 231 | — | 2 | 0.553 | 0.008 | 0.156 | 6.8(−7) |
| 1.00 | 1 | 0.0037 | 160 | — | — | 160 | — | 2 | 0.577 | 0.008 | 0.193 | 1.2(−6) |
| 1.16 | 1 | 0.0058 | 142 | — | 83 | 225 | 3 | 3 | 0.583 | 0.009 | 0.355 | 1.6(−6) |
| 1.20 | 1 | 0.0062 | 138 | — | 103 | 241 | 4 | 4 | 0.585 | 0.009 | 0.396 | 1.6(−6) |
| 1.50 | 1 | 0.0076 | 124 | 88 | 157 | 369 | 4 | 5 | 0.589 | 0.010 | 0.719 | 2.0(−6) |
| 2.50 | 1 | 0.0084 | 329 | 84 | 467 | 881 | 7 | 12 | 0.617 | 0.022 | 1.740 | 2.0(−6) |
| 3.00 | 1 | 0.0086 | 302 | 160 | 603 | 1065 | 8 | 16 | 0.627 | 0.025 | 2.093 | 2.0(−6) |
| 5.00 | 1 | 0.0087 | 152 | 3.3 | 14.8 | 170 | 47 | 51 | 0.918 | 0.016 | 2.228 | 1.3(−5) |
| 1.30 | 2 | 0.0068 | 288 | — | — | 288 | — | 4 | 0.592 | 0.016 | 0.498 | 1.7(−6) |
| 1.40 | 2 | 0.0072 | 299 | — | 28 | 327 | 5 | 5 | 0.594 | 0.016 | 0.605 | 1.9(−6) |
| 1.50 | 2 | 0.0076 | 206 | 88 | 68 | 362 | 5 | 5 | 0.595 | 0.016 | 0.713 | 2.0(−6) |
| 2.00 | 3 | 0.02 | 510 | — | 46 | 556 | 8 | 8 | 0.588 | 0.026 | 1.255 | 2.2(−6) |
| 2.50 | 3 | 0.02 | 602 | 89 | 162 | 853 | 10 | 11 | 0.597 | 0.035 | 1.752 | 2.0(−6) |
| 3.00 | 3 | 0.02 | 780 | 86 | 260 | 1126 | 12 | 15 | 0.599 | 0.037 | 2.121 | 1.9(−6) |
| 2.00 | 4 | 0.02 | 417 | — | 9.9 | 427 | 7 | 7 | 0.582 | 0.020 | 1.236 | 2.9(−6) |
| 2.50 | 4 | 0.02 | 602 | — | 44.2 | 646 | 9 | 9 | 0.589 | 0.027 | 1.703 | 2.6(−6) |
| 3.00 | 4 | 0.02 | 693 | 87 | 38.7 | 819 | 11 | 11 | 0.593 | 0.031 | 2.015 | 2.5(−6) |

*Notes*: Listed are the initial mass ($M_\odot$), the model number, the metallicity $Z$, the lifetime of the M, S, C and the total AGB phase in $10^3$ yr, the pulse number at which a star became a carbon star, the total number of pulses on the AGB, the final mass, the core growth on the AGB, the total mass lost on the AGB (all in $M_\odot$) and the average mass loss rate on the AGB (in $M_\odot$ yr$^{-1}$).
Model 1: The final LMC model with $M_c^{min} = 0.58 M_\odot$, $\lambda = 0.75$, $\eta_{AGB} = \eta_{EAGB} = 5$, including hot bottom burning.
Model 2: As model 1 with $M_c^{min} = 0.59 M_\odot$, $\lambda = 0.70$.
Model 3: As model 1 but with $Z = 0.02$.
Model 4: As model 3 and with $\eta_{AGB} = \eta_{EAGB} = 7$.

Based upon the observed relative numbers of Cepheids and bright AGB stars, Reid et al. (1990) concluded that the average lifetime of luminous ($M_{bol} < -6$) AGB stars is "no more than 2 $10^5$ yrs". Hughes & Wood (1990) and Iben (1991) derive a similar lifetime. Our calculations confirm this. In our model a $5M_\odot$ star spends 1.3 $10^5$ yr below $M_{bol} = -6$. This agreement supports our derived (high) mass loss rates.

Blanco & McCarthy (1983) have estimated the number of carbon stars in the LMC. They derived a number of $\approx$11 000 over an area $\approx$100 deg$^2$. The area they considered includes the outskirts of the LMC, and is much larger than that considered by others. Because we want to compare the number of AGB stars with the LPV census of Hughes (1989) in a future paper, we estimated the number of carbon stars in the area surveyed by Hughes for LPV ($\sim$55 deg$^2$), based on the isopleths of Blanco & McCarthy. This area includes all carbon stars within the 75 deg$^{-2}$ isopleth ($\sim$7000 carbon stars) plus a large area within the 25 deg$^{-2}$ isopleth. The total number of carbon stars within the area surveyed by Hughes for LPV is estimated to be 8250$\pm$250. In Sect. 3 we estimated that 10% of all carbon stars are low-luminosity J-type stars which may not be on the AGB, but possibly related to the R-type carbon stars observed in the Galaxy. The number of carbon stars on the AGB is estimated to be 7500$\pm$500. From Table 5 we find an average carbon star lifetime of (2.0$\pm$0.5) $10^5$ yr. We conclude that the birth rate of carbon stars on the AGB in the LMC equals $dN/dt \approx N/T = 0.038 \pm 0.010$ yr$^{-1}$.

For the oxygen-rich AGB stars a similar estimate can be made. The observed C/M ratio is between 0.4 and 2 depending on the spectral type included in counting M-stars (Blanco & McCarthy 1983). Assuming our model result of C/M = 0.85 with an error of 0.2 (based on a possibly spread of 0.02 in $M_c^{min}$) we derive a number of 6700–12 300 oxygen-rich AGB stars. With a mean lifetime of (1.6$\pm$0.3) $10^5$ yr (Table 5), we derive a birth rate of 0.058 yr$^{-1}$ within a factor of 1.6 (i.e. 0.035–0.095 yr$^{-1}$).

An independent estimate can be made by realising that the carbon star birth rate equals the AGB death rate in the range $\sim$1.2–$\sim$3.5$M_\odot$. Based on the adopted IMF and SFR we derive that the number of stars in the $\sim$1.2–$\sim$3.5$M_\odot$ range is between 40% and 60% of all stars in the range $\sim$0.93–$\sim$8$M_\odot$, depending on the exact values of the mass limits. Therefore we derive a birth rate of AGB stars of 0.076 yr$^{-1}$ within a factor of 1.6 (i.e. 0.047–0.122 yr$^{-1}$). A birth rate of AGB stars of 0.07$\pm$0.02 yr$^{-1}$ is consistent with both estimates.

Payne-Gaposhkin (1971) identified 1111 Cepheids in a 55 deg$^2$ area in the LMC. This survey is incomplete, possibly up to a factor of 4 (Wright & Hodge 1971). Becker et al. (1977) derived a number of 2000 Cepheids. Assuming the LMC contains 2000 Cepheids within a factor of 2 and a mean lifetime of the Cepheid phase of 2–5 $10^5$ yr (Becker et al. 1977) we derive a birth rate of 3–5$M_\odot$ stars of 6.3 $10^{-3}$ yr$^{-1}$. From the adopted IMF and SFR it is deduced that the number of stars in the range 0.93–8$M_\odot$ to the number of 3–5$M_\odot$ stars is between 12 and 22 depending on the exact value of the mass limits. Based on the

number of Cepheids we estimate a birth rate of AGB stars of $0.10\ yr^{-1}$ uncertain to a factor of 2.2 (i.e. 0.045–0.22 $yr^{-1}$).

Hardy et al. (1984) identified $2100 \pm 210$ clump stars in a 6′ by 12′ region in the NW part of the bar in the LMC. From Lattanzio (1991) we find a mean lifetime of $(1.5 \pm 0.5)\ 10^8$ yr for the clump phase. Boldly extrapolating to the whole LMC ($55 \pm 5\ deg^2$) we estimate an evolution rate of clump stars of $0.11 \pm 0.04\ yr^{-1}$.

Jacoby (1980) estimated the total number of PN in the LMC to be $996 \pm 253$. A number of possible PN included in Jacobys calculation were subsequently shown not to be PN (Boroson & Liebert 1989). Repeating Jacoby's analysis taking these new results into account (in particular $N_J = 25$, $f_1 = 2.19$ in Jacoby's formula) gives an improved number of $838 \pm 212$ PN in the LMC. Using a mean lifetime of 2–5 $10^4$ yr results in a birth rate of PN of $0.026\ yr^{-1}$ uncertain to a factor of 2 (i.e. 0.013–0.052 $yr^{-1}$).

We conclude that the calculated lifetimes of AGB stars from our standard model, in combination with the observed number of carbon and oxygen-rich stars gives a birth rate of $0.07 \pm 0.02\ yr^{-1}$, which is in good agreement with the AGB evolution rates estimated from the number of clump stars ($0.11 \pm 0.04\ yr^{-1}$) and Cepheids ($0.10\ yr^{-1}$ within a factor of 2.2). The estimated birth rate of PN ($0.026\ yr^{-1}$ within a factor of 2) is well below this value which suggests that a fairly large number of low-mass stars ($M_{\rm initial} \lesssim 1.1 M_\odot$) either do not become PN (evolution probably too slow) or have simply not been detected yet.

Our model predicts that in the LMC stars more massive than $1.2 M_\odot$ will pass through a carbon star phase and stars more massive than $1.5 M_\odot$ pass through an S-star phase. If the transition from M to S star occurs at C/O = 0.90 instead of 0.81 the latter value would be $\sim 1.7 M_\odot$. These numbers depend on the minimum core mass for dredge-up and the dredge-up efficiency. For $M_{\rm c}^{\rm min} = 0.59 M_\odot$ and $\lambda = 0.7$ only stars $> 1.4 M_\odot$ pass through the carbon star phase. We have compared our results with the observations of AGB stars in LMC clusters (Frogel et al. 1990; Westerlund et al. 1991a). They report that S-stars are observed in LMC clusters of SWB (Searle et al. 1980) type IV and V but not in type VI and VII. Carbon stars are predominately observed in clusters of type IV, V and VI with very few in type I–III. There is no known LMC cluster of type VII containing a carbon star. The oldest LMC clusters containing carbon stars (N 1978, N 2173) have ages between 2–3 Gyr (Sagar & Pandey 1989). Interpolating in the models of Sweigart et al. (1989) and Lattanzio (1991) this corresponds to stars that are on the AGB of initial mass between $1.3 M_\odot$ and $1.6 M_\odot$. This is in good agreement with our prediction. Our result that stars need to be somewhat more massive to go through an S-star phase is consistent with the fact that they are observed in clusters of earlier SWB type. The fact that there are few or no C and S stars in young clusters of SWB type I–III, corresponding to initial masses $\gtrsim 4 M_\odot$, is also in agreement with our predictions.

In comparing the solar metallicity models 3 and 4 with the LMC model 1, we note that the minimum mass for carbon star formation is raised to $\approx 2 M_\odot$. For every initial mass the duration of the carbon star phase is shorter for the $Z = 0.02$ models than for the corresponding LMC models. This is of course consistent with the fact the C/M ratio in the Galaxy is lower than in the LMC.

From a comparison of model 3 and 4 we stress the importance of the mass loss rate on the AGB in determining the lifetimes of AGB stars in general and the carbon stars in particular. For model 4, which may be indicative for the solar neighbourhood, we see that stars become carbon stars at the last TP on the AGB and that the carbon star phase lasts a few times $10^4$ years. This number is in surprisingly good agreement with the lifetime estimate of the carbon star phase in the solar neighbourhood made by Groenewegen et al. (1992).

*Acknowledgements.* It is a pleasure to thank Bobby van den Hoek and Sander Slijkhuis for stimulating discussions and a critical reading of earlier versions of this paper. The research of MG is supported under grant 782-373-030 by the Netherlands Foundation for Research in Astronomy (ASTRON), which is financially supported by the Netherlands Organisation for Scientific Research (NWO).

## Appendix A: hot bottom burning

Hot bottom burning (HBB) has been described in detail by Sugimoto (1971), Uus (1973), Iben (1973), Scalo et al. (1975), RV and Sackmann & Boothroyd (1991). These authors do not agree on the exact extent of HBB. This is due to uncertainties in the temperature at the base of the convective envelope, $T_{\rm B}$, which is quite sensitive to the core and total mass and to the mixing-length. In light of these uncertainties we restricted ourselves to a simple model of HBB, which reproduces the results of RV fairly well. In order to make headway we have only considered the $\alpha = 2$ case of RV for three reasons. Firstly, RV gives information on $T_{\rm B}$ only for this case. Secondly, a mixing-length parameter of 2 seems more appropriate than the values considered by RV (see e.g. Maeder & Meynet 1989) and thirdly, it will enable us to study the maximum effect of HBB on the results.

In our simple model to describe HBB four parameters are needed: (1) the (average) temperature at the base of the convective envelope, $T_{\rm B}$, as a function of core and total mass, (2) the fraction ($f_{\rm HBB}$) of newly dredged up matter exposed to the high temperatures at the bottom of the envelope, (3) the amount of matter in the envelope, relative to the total envelope mass, which is mixed down and processes at the bottom of the envelope ($f_{\rm bur}$) and (4) the (average) exposure time, $t_{\rm HBB}$, of matter in the zone of HBB. The temperature at the base of the convective envelope is an important quantity since only for $T_{\rm B} \gtrsim 30\ 10^6$ K significant HBB occurs (RV). When $T_{\rm B} \lesssim 30\ 10^6$ K the lifetimes of the species involved in the CNO-cycle against proton capture are too long.

The value of $T_{\rm B}$, appropriate for the $\alpha = 2$ case of RV was derived from Figs. 4–6 of RV, where they list the values of $T_{\rm B}$ at different luminosities for different masses. Transforming the luminosities into core masses using the core–mass–luminosity relation of RV, we have approximated $T_{\rm B}$ as a function of total and core mass. We find (temperatures in $10^6$ K)

$$T_{\rm B} = T_{\rm B}^0 + 127.6\ (M_{\rm c} - 0.8), \tag{A1}$$

where the zeropoint is initial mass dependent:

$$T_{\rm B}^0 = -25.45 + 16.41\ M_{\rm initial}. \tag{A2}$$

Iben (1976) quotes $T_{\rm B} = 44 + 100\ (M_{\rm c} - 0.8)$ for a $M = 7 M_\odot$ model derived with $\alpha_{\rm Iben} = 0.7$. The slopes of the two relations compare fairly well and the difference in the zeropoint is due to the difference in the mixing-length parameter.

Equation (A1) is valid until the envelope mass is reduced below a critical value, after which $T_{\rm B}$ drops significantly below the value given by Eq. (A1). The critical envelope mass is denoted

by $M_{\rm env}^{\rm HBB}$. Another important quantity is the total effective exposure time of matter to the high temperatures ($t_{\rm HBB}$). If $t_{\rm ip}$ is the interpulse period and if a hump of matter spends a time $t_1$ in the HBB-zone due to the convective motion, and a time $t_2$ in the cooler outer parts of the envelope, this hump of matter will be mixed approximately $t_{\rm ip}/t_1+t_2$ times through the HBB-zone during an interpulse period. Therefore the total time a hump of matter is exposed to the high temperatures during the interpulse period is roughly given by $t_{\rm HBB}=t_1/(t_1+t_2)\ t_{\rm ip}$. We have not made an effort to try to determine $t_1$ and $t_2$ from first principle, but rather determined the ratio $f=t_1/(t_1+t_2)$ by fitting our model to the results of RV. However, since the region of high temperatures is small compared to the extent of the total envelope only $f\ll 1$ would be a physical meaningful result.

The fraction, $f_{\rm HBB}$, of newly dredged-up material processed by HBB is expected to be close to 1. Since, the dredged-up material is forced through the bottom of the convective envelope, only a small fraction can escape HBB, through the help of convective motion.

We implemented the algorithms used by RV and compared our model results with those of the RV model $\alpha=2$ case ($Z=0.02$, $Y=0.28$, $\eta=1/3$, case A) to determine the values of $t_{\rm HBB}$, $f_{\rm HBB}$ and $f_{\rm bur}$. We constructed a grid in these parameters and after some experimenting we found good results for combinations of parameters in the range: $0.0010\ t_{\rm ip} \le t_{\rm HBB} \le 0.0020\ t_{\rm ip}$, $0.93 \le f_{\rm HBB} \le 0.95$ and $2\,10^{-4} \le f_{\rm bur} \le 3\,10^{-4}$. By comparing both lifetimes and yields, the most suitable parameters for the $\alpha=2$ model of RV are: $t_{\rm HBB}=0.0014\ t_{\rm ip}, f_{\rm HBB}=0.94, f_{\rm bur}=3\ 10^{-4}$. By comparing our model to the "case B" model of RV we found that $M_{\rm env}^{\rm HBB}=0.85\ M_{\rm pn}$,[2] gives very good results, except for $M=3.3M_\odot$. We are left with a discussion on the method to calculate the time evolution of the species involved in the CNO-cycle. We used the method presented in Clayton (1968). The basic assumption in his method is that the two reaction chains of the CNO-cycle, the CN-cycle,

$$^{12}{\rm C(p,\gamma)^{13}\,N(e^+,\nu)^{13}\,C(p,\gamma)^{14}\,N(p,\gamma)^{15}\,O(e^+,\nu)^{15}\,N(p,\alpha)^{12}\,C} \quad \text{(A3)}$$

and the ON-cycle,

$$^{15}{\rm N(p,\gamma)^{16}\,O(p,\gamma)^{17}\,F(e^+,\nu)^{17}\,O(p,\alpha)^{14}\,N} \quad \text{(A4)}$$

can be separated. This is due to the fact that the $^{15}$N(p, $\gamma$) reaction occurs about once every 2800 $^{15}$N(p, $\alpha$) reactions.

After some simplifications (see Clayton 1968) the evolution of the CN and ON-cycle is reduced to an eigenvalue problem in the ($^{12}$C, $^{13}$C, $^{14}$N) and ($^{14}$N, $^{16}$O, $^{17}$O) abundances respectively. The eigenvectors depend on the initial values of the abundances and the eigenvalues depend on the lifetimes of the species against proton captures. We used the reaction rates of Fowler et al. (1975) to calculate the reaction rates. We verified the method of Clayton by comparing the results to the exact time-dependent calculations of Caughlan (1965), using identical initial conditions and nuclear lifetimes. The differences in the abundances are less than 1%, which is similar to the accuracy claimed by Clayton.

In our model we do not need the abundances at a specific time but rather the averaged abundance $1/t\int_0^t X(t)\,{\rm d}t$, see Eqs. (35) and (36). In the method of Clayton the evolution of a species $X$ is of the simple form $X(t)=\sum_{i=1}^{3} U_i {\rm e}^{\lambda_i t}$, so the average abundance can be calculated analytically.

[2] The value of $M_{\rm pn}$ is given by RV's Eq. (33).

## Appendix B: AGB lifetimes

The distribution of stars on the AGB [Eq. (37)] depends on the lifetime of stars on the AGB, $t_{\rm AGB}$. We expect the AGB lifetimes to depend primarily on the mass loss rate on the AGB. We calculated $t_{\rm AGB}$ for a sequence of stars with $\eta_{\rm AGB}=1$, 5, 10 (solid, long dashed, dot-dashed in Fig. B1 respectively). For a given initial mass, the pre-AGB lifetimes of Iben & Laughlin (1989) were used to derive its age, and the age–metallicity relation of the LMC of van den Hoek & de Jong (1992) to derive $Z$. The helium abundance was calculated from Eq. (24). For other relevant parameters we used our standard model. The results are displayed in Fig. B1, where we normalised $t_{\rm AGB}$ to its value of the $3M_\odot$ model.

The shape of the $t_{\rm AGB}$ function is rather peculiar and deserves some further attention. It could be expected that $t_{\rm AGB}$ is an increasing function of initial mass, simply because there is more envelope mass available. Evidently this is not true. First of all, for stars of high enough mass, the AGB is terminated when the core mass reaches the Chandrasekhar mass. Therefore, the lifetime is determined by the time the core mass grows from $M_{\rm c}(1)$ to $M_{\rm Ch}$. This is (almost) independent of envelope mass and therefore constant (in absolute terms). Because the lifetime of the reference $3M_\odot$ model decreases with increasing $\eta_{\rm AGB}$, the high mass points for $\eta_{\rm AGB}=5$ and 10 lie above the $\eta_{\rm AGB}=1$ curve. The value of $\eta_{\rm AGB}$ does determine however which stars live long enough to reach the Chandrasekhar mass. The transition from stars that end as white dwarfs and those who end as supernova is reflected in the peaks in the $\eta_{\rm AGB}=1$ (at $M=4.5M_\odot$) and $\eta_{\rm AGB}=5$ (at $M=7.5M_\odot$) curves.

For stars below $2M_\odot$, the mass loss on the RGB becomes increasingly important in determining the AGB lifetimes. For decreasing mass this means less envelope mass and lower lifetimes. For the lowest mass stars the lifetime increases suddenly. This is a metallicity effect as demonstrated in Fig. B1 where we plotted the results for $\eta_{\rm AGB}=5$ for a set of models following the age–metallicity relation (long dashed curve) and for a constant metallicity (short dashed). Down to $M\approx 1.5M_\odot$ the two curves

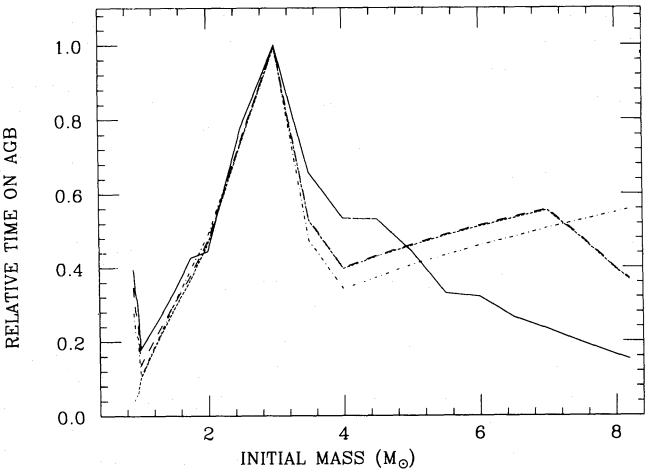


**Fig. B1.** The relative lifetimes of stars on the AGB, for a mass loss parameter $\eta_{\rm AGB}=1$ (solid), 5 (long dashed), 10 (dotted). The upturn at the lowest masses is a metallicity effect. The shape of the curve at the highest masses is determined by the time to reach the Chandrasekhar mass. The short-dashed curve represents $\eta_{\rm AGB}=5$ with constant metallicity. Details are given in Appendix B

are identical. For stars below $\sim 1 M_{\odot}$ the metallicity drops very fast with decreasing initial mass due to the age–metallicity relation. The mass loss on the RGB increases with decreasing mass but also decreases with decreasing metallicity (see Table 2). For the lowest mass stars the metallicity effect compensates the mass effect. There is (relative) more envelope mass available and the lifetime increases. When the calculations are extended to even lower initial masses, the AGB lifetimes increase a bit further and then drop to 0, for the star which has lost so much mass on the RGB that $M_{\rm env}=0$ at the start of the AGB. From Fig. B1 we see that for stars with $M \lesssim 4 M_{\odot}$ the influence of $\eta_{\rm AGB}$ on the relative AGB lifetimes is negligible and even for high mass stars the effect is small. Because some preliminary calculations indicated that $\eta_{\rm AGB} > 1$ was needed to fit the observed carbon star LF in the LMC the following approximation to the curves in Fig. B1 was used:

$$t_{\rm AGB}(M)/t_{\rm AGB}(3) = \begin{cases} -2.061\,M + 2.197, & 0.93 < M < 1, \\ 0.336\,M - 0.199, & 1 < M < 2, \\ 0.528\,M - 0.584, & 2 < M < 3, \\ -0.937\,M + 3.812, & 3 < M < 3.56, \\ 0.48, & 3.56 < M < 8.2. \end{cases}$$

This approximation was used in all calculations reported in this paper.

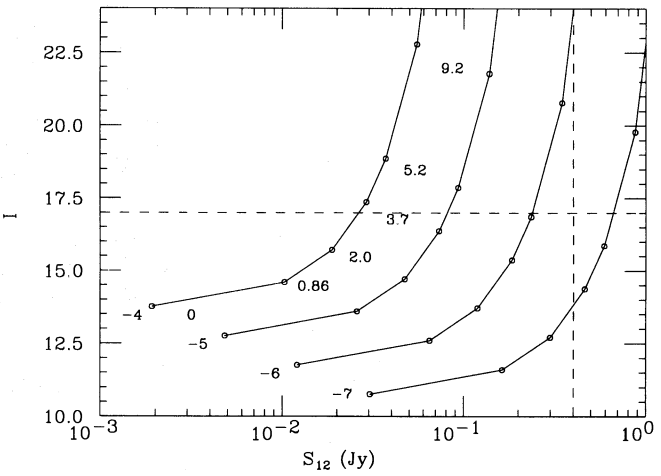


**Fig. C1.** The $I$ magnitude and IRAS 12 $\mu$m flux for stars in the LMC surrounded by a carbon-rich dust shell. Indicated are the curves for $M_{\rm bol} = -4, -5, -6, -7$ and various optical depths at 0.8 $\mu$m. Numerical details are given in Appendix C. From this diagram we conclude that it is possible that optically invisible carbon stars ($I > 17$) are not detected by IRAS ($S_{12} < 0.4$ Jy)

## Appendix C: obscuration of AGB stars

The carbon star LF (Fig. 5) which is used in this study was derived from optical surveys which are complete down to $I \approx 17$. It is obvious that a star in the LMC which is losing mass at a considerable rate and is surrounded by a dust shell, could, in principle be weaker than $I = 17$. On the other hand, such a star may be detected by IRAS at 12 $\mu$m.

In this appendix we derive an upperlimit to the number of carbon stars missed by the optical surveys and show that it is possible that a carbon star which is fainter than $I = 17$ would *not* be detected by IRAS. We further discuss at which mass loss rate a star would become fainter than $I = 17$ in the LMC.

Would all carbon stars that are fainter than $I = 17$ be detected by IRAS? To answer this question some radiative transfer calculations were performed. The standard model was a star of $T_{\rm eff} =$ 3000 K, L = 20 000$L_{\odot}$ ($M_{\rm bol} \approx -6$) at a distance of 50.2 kpc surrounded by a dust shell. The shape of the spectrum is determined by the optical depth as a function of wavelength:

$$\tau_{\lambda} \propto \frac{\dot{M}\,\Psi\,Q_{\lambda}/a}{R_{*} r_{\rm in} v_{\infty} \rho}, \qquad \text{(C1)}$$

where $\dot{M}$ is the mass loss rate, $\Psi$ the dust-to-gas ratio, $Q_{\lambda}$ the extinction coefficient, $a$ the grain radius, $R_{*}$ the stellar radius in solar units, $r_{\rm in}$ the inner radius of the dust shell in stellar radii, $v_{\infty}$ the expansion velocity and $\rho$ the grain density. Equation (C1) assumes a $1/r^2$ density law. The standard values were $\Psi = 0.003$, $v_{\infty} = 15$ km s$^{-1}$, $\rho = 3.3$ g cm$^{-3}$. The inner radius was calculated selfconsistently by assuming a temperature at the inner radius ($T_{\rm c}$) of 1500 K. For the grains we assumed AC amorphous carbon (Bussoletti et al. 1987) with $Q_{\lambda}/a = 213\,000$ cm$^{-1}$ at 0.8 $\mu$m.[3] We did not consider silicon carbide because it has become clear that this is a trace species ($\lesssim 10\%$) in the dust shells of galactic carbon stars relative to amorphous carbon. In the LMC with its lower metallicity there should be even less silicon to form SiC.

We ran a series of models with increasing mass loss rate and calculated the $I$ magnitude and the IRAS flux at 12 $\mu$m (folded with the detector response of IRAS). The results are plotted in Fig. C1. Indicated are the curves for $M_{\rm bol} = -4, -5, -6$ and $-7$. Along the $M_{\rm bol} = -4$ curve the optical depth at 0.8 $\mu$m is indicated for the $L = 20\,000 L_{\odot}$, $T_{\rm eff} = 3000$ K model. For the standard parameters this corresponds to mass loss rates of 0, 2 $10^{-7}$, 5 $10^{-7}$, 1 $10^{-6}$ 1.5 $10^{-6}$ and 3 $10^{-6} M_{\odot}$ yr$^{-1}$. The mass loss rate does not scale exactly linear with the optical depth because of radiative transfer effects. For higher mass loss rates the backwarming of the grains becomes important so the assumed condensation temperature of 1500 K is reached at a greater distance.

For any point in the diagram the mass loss scales with $\sqrt{L/20\,000}/(T_{\rm eff}/3000)^2$ due to the dependence of the optical depth on the stellar radius and approximately like $(T_{\rm eff}/T_{\rm c})^{(4+p)/2}$ due to the dependence of the optical depth on the inner radius. The parameter $p$ gives the overall wavelength dependence of the grains, $Q_{\lambda} \sim \lambda^{-p}$, and equals $\sim 1$ for amorphous carbon. For example, from Fig. C1 we derive that a star of $M_{\rm bol} = -4$ becomes invisible at $I$ at $\tau \approx 3.3$. If we assume a stellar temperature of 3500 K this corresponds to a mass loss rate of (3.3/3.7) 1.0 $10^{-6}$ $\sqrt{(3080/20\,000)(3500/3000)} = 3.7\ 10^{-7} M_{\odot}$ yr$^{-1}$.

Important to the synthetic evolution models is to know the mass loss rate at which a carbon star becomes optically invisible. We expect the flux in the optical to vary like

$$\frac{c\,L}{4\pi D^2} e^{-\tau} = f_{\rm lim},$$

where $c$ is some constant, $L$ the total luminosity, $D$ the distance, $\tau$ the optical depth and $f_{\rm lim}$ the flux. This can be recast into

$$M_{\rm bol} = a - b\,\tau.$$

[3] Actually we multiplied the value of $Q_{\lambda}/a$ given by Bussoluetti et al. by a factor of 5 to let their results agree with those of Koike et al. (1980).

We have made a fit using the results of our radiative transfer models and found that a carbon star in the LMC becomes fainter than $I=17$ at a mass loss rate

$$\dot{M}=F_{\rm IR}\frac{-1.49-M_{\rm bol}}{2.79\ 10^{6}}\sqrt{L/20\,000}\sqrt{T_{\rm eff}/3000.} \qquad \text{(C2)}$$

The change in the critical mass loss rate due to the luminosity effect alone is a factor of 4.6 going from $M_{\rm bol}=-4$ to $-6$. The scale factor $F_{\rm IR}$ includes the uncertainties in $v_\infty$, $\rho$, $Q_\lambda/a$, $r_{\rm in}$ and particularly the dust-to-gas ratio $\Psi$, which is poorly known in the LMC. Assuming a dust-to-gas ratio in the LMC between 1/700 and 1/1500 (Schwering 1988), terminal velocities which can be up to a factor of 3 lower than in the Galaxy (Wood 1987) and random errors in $\rho$, $r_{\rm in}$ and $Q_\lambda/a$ of factors of 2, 2 and 5 respectively, an observational constraint of $0.04<F_{\rm IR}<100$ can be set.

Similar radiative transfer calculations were made for oxygen-rich stars. Astronomical silicate (Draine & Lee 1984 and unpublished work) was used with $Q_\lambda/a=13\,230\ {\rm cm}^{-1}$ at 9.5 μm, $p=2$ and a condensation temperature of $T_{\rm c}=1000$ K. For the terminal velocity, the dust-to-gas ratio and the grain density the same values as for the carbon stars were used. We find that an oxygen-rich star becomes fainter than $I=17$ in the LMC at a mass loss rate

$$\dot{M}=F_{\rm IR}\frac{-1.73-M_{\rm bol}}{2.19\ 10^{4}}\sqrt{L/20\,000}\,(T_{\rm eff}/3000). \qquad \text{(C3)}$$

In the synthetic evolution models Eq. (C2) was used for the carbon and S-stars and Eq. (C3) for the M-stars to determine at each timestep if a star was visible or obscured. The factor $F_{\rm IR}$ in Eqs. (C2) and (C3) as assumed to be equal.

Reid et al. (1990) combined IRAS data (down to $S_{12}=0.1$ Jy) with $V$ and $I$ plates of a 9.3 deg$^2$ area in the LMC. Out of a total of 156 IRAS detections 63 had the characteristics of a stellar photosphere or a circumstellar shell. After removing 17 foreground objects and 17 LMC supergiants they were left with 13 AGB candidates and 16 IRAS sources with no obvious optical counterpart. The 13 AGB candidates have $11.1<I<15.7$ and therefore would have been found by the optical surveys. There remain 1.7 deg$^{-2}$ sources with $S_{12}>0.1$ Jy and $I>17$.

The IRAS survey was essentially complete down to $S_{12}=0.4$ Jy at 12 μm (*Explanatory Supplement* 1986, Chapter VIII). Of the 16 unidentified sources only 2 have $S_{12}>0.4$ Jy ($\sim 0.2$ deg$^{-2}$). From Fig. C1 we derive that IRAS could have missed obscured carbon stars with $S_{12}>0.4$ Jy when $M_{\rm bol}\gtrsim -6$. There are $\sim 7$ deg$^{-2}$ optical carbon stars brighter than $M_{\rm bol}=-6$. If we assume that the unidentified sources are all carbon stars and all are brighter than $M_{\rm bol}=-6$ we derive an upperlimit of $\sim 3\%$ obscured carbon stars brighter than $M_{\rm bol}=-6$.

In Sect. 3.3 where the influence of the mass loss rate and obscuration is investigated we proceeded in the following way. For a given mass loss rate $\eta_{\rm AGB}$, Eqs. (C2) and (C3) were applied with the scale factor $F_{\rm IR}$ varied in such a way that 3% of the carbon stars brighter than $M_{\rm bol}=-6$ were obscured. The model then provides information on the degree of obscuration at other luminosities.

## References


Anders E., Grevesse N., 1989, Geochim. Cosmochim. Acta 53, 197

Barbuy B., Milone A., Spite M., Spite F., 1991, in: Hayes R., Milne D. (eds.) The Magellanic Clouds. Reidel, Dordrecht, p. 370

Barlow M.J., 1989, in: Torres-Peimbert S. (ed.) Planetary Nebulae, Kluwer, Dordrecht, p. 319

Becker S.A., Iben I., 1979, ApJ 232, 831 (BI1)

Becker S.A., Iben I., 1980, ApJ 237, 111 (BI2)

Becker S.A., Iben I., Tuggle R.S., 1977, ApJ 218, 633

Bedijn P., 1988, A&A 205, 105

Blanco V.M., McCarthy M.F., 1981, in: Iben I., Renzini A. (eds.) Physical Processes in Red Giant Stars. Kluwer, Dordrecht, p. 147

Blanco V.M., McCarthy M.F., 1983, AJ 88, 1442

Blanco V.M., McCarthy M.F., Blanco B.M., 1980, ApJ 242, 938

Blöcker T., Schönberner D., 1990, A&A 240, L11

Blöcker T., Schönberner D., 1991, A&A 244, L43

Boothroyd A.I., Sackmann I.-J., 1988a, ApJ 328, 632 (BS1)

Boothroyd A.I., Sackmann I.-J., 1988b, ApJ 328, 641 (BS2)

Boothroyd A.I., Sackmann I.-J., 1988c, ApJ 328, 653 (BS3)

Boothroyd A.I., Sackmann I.-J., 1988d, ApJ 328, 671 (BS4)

Boroson T.A., Liebert J., 1989, ApJ 339, 844

Brown J.A., Smith V.V., Lambert D.L., Dutchover E., Hinkle K.H., Johnson H.R., 1990, AJ 99, 1930

Bryan G.L., Volk K., Kwok S., 1990, ApJ 365, 301

Bussoletti E., Colangeli L., Borghesi A., Orofino V., 1987, A&AS 70, 257

Castellani V., Chiefi A., Straniero O., 1990, ApJS 74, 463

Caughlan G.R., 1965, ApJ 141, 688

Chiosi C., Bertelli G., Bressan A., 1987, in: Azzopardi M., Matteuci F. (eds.) Stellar Evolution and Dynamics of the Outer Halo of the Galaxy. ESO, Garching, p. 415

Clayton D., 1968, Principles of Stellar Evolution and Nucleosynthesis, McGraw-Hill, New York, p. 390

Clegg R.E.S., 1991, in: Michaud G., Tutukov A. (eds.) Proc. IAU Symp. 145, Evolution of Stars, Reidel, Dordrecht, p. 387

Cohen J.G., Frogel J.A., Persson S.E., Elias J.H., 1981, ApJ 249, 481

Cox A.N., Steward J.N., 1970, ApJS 19, 243

de Jong T., 1990, in: Mennessier M.O., Omont A. (eds.) From Miras to planetary Nebulae. Editions Frontieres, Gif-sur Yvette, p. 289

Dopita M.A., Meatheringham S.J., 1990, ApJ 357, 140

Dopita M.A., Meatheringham S.J., 1991, ApJ 367, 115

Draine B.T., Lee H.M., 1984, ApJ 285, 89

Fowler W.A., Caughlan G.R., Zimmerman B.A., 1975, ARA&A 13, 69

Frantsman Yu. L., 1986, Afz 24, 131

Frogel J.A., Richer H.B., 1983, ApJ 275, 84

Frogel J.A., Cohen J.G., Persson S.E., Elias'J.H., 1981, in: Iben I., Renzini A. (eds.) Physical Processes in Red Giants Stars. Reidel, Dordrecht, p. 159

Frogel J.A., Mould J., Blanco V.M., 1990, ApJ 352, 96

Grevesse N., 1991 in: Michaud G., Tutokov A. (eds.) The evolution of stars. Reidel, Dordrecht, p. 63

Groenewegen M.A.T., de Jong T., Van der Bliek N.S., Slijkhuis S., Willems F.J., 1992, A&A 253, 150

Hamada T., Salpeter E.E., 1961, ApJ 134, 683

Hardy E., Buonanno R., Corsi C.E., Janes K.A., Schommer R.A., 1984, ApJ 278, 592

Hollowell D.E., 1987, in: Kwok S., Pottasch S.R. (eds.) Late Stages of Stellar Evolution. Reidel, Dordrecht, p. 239

Hollowell D.E., 1988, Ph.D. Thesis, University of Illinois
Hughes S.M.G., 1989, AJ 97, 1634
Hughes S.M.G., Wood P.R., 1990, AJ 99, 784
Iben I., 1973, ApJ 185, 209
Iben I., 1975, ApJ 196, 525
Iben I., 1976, ApJ 208, 165
Iben I., 1977, ApJ 217, 788
Iben I., 1981, ApJ 246, 278
Iben I., 1982, ApJ 260, 821
Iben I., 1985, QJRAS 26, 1
Iben I., 1988, in: Blanco V.M., Philips M.M. (eds.) Astr. Soc. of the Pacific Conf. Ser. Vol. 1, Progress and Opportunities in Southern Hemisphere Optical Astronomy, p. 220
Iben I., 1991, in: Michaud G., Tutukov A. (eds.) Evolution of stars. Kluwer, Dordrecht, p. 257
Iben I., Laughlin G., 1989, ApJ 341, 312
Iben I., Renzini A., 1983, ARA&A 21, 271 (IR)
Iben I., Truran J.W., 1978, ApJ 220, 980 (IT)
Iben I., Tutukov A.V., 1989, in: Torres-Peimbert S. (ed.) Planetary Nebulae, Kluwer, Dordrecht, p. 505
Jacoby G.H., 1980, ApJS 42, 1
Jacoby G.H., Walker A.R., Ciardullo R., 1990, ApJ 365, 471
Kippenhahn R., 1981, A&A 102, 293
Koester D., Weidemann V., 1985, A&A 153, 260
Koike C., Hasegawa H., Manabe A., 1980, Ap&SS 67, 495
Kudritzki R.P., Pauldrach A., Puls J., 1987, A&A 173, 293
Lambert D.L., 1991, Observational Effects of Nucleosynthesis in Evolved Stars, preprint
Lattanzio J.C., 1986, ApJ 311, 708
Lattanzio J.C., 1987a, ApJ 313, L15
Lattanzio J.C., 1987b, in: Kwok S., Pottasch S.R., (eds.) Late Stages of Stellar Evolution. Reidel, Dordrecht, p. 235
Lattanzio J.C., 1989a, ApJ 344, L25
Lattanzio J.C., 1989b, in: Johnson H.R., Zuckerman B. (eds.) Evolution of Peculiar Red Giant Stars. Cambridge Univ. Press, Cambridge, p. 161
Lattanzio J.C., 1989c, ApJ 347, 989
Lattanzio J.C., 1991, ApJS 76, 215
Lequeux J., 1990, in: Mennessier M.O., Omont A. (eds.) From Miras to Planetary Nebulae. Editions Frontieres, Gif-sur-Yvette, p. 271
Lundgren K., 1988, A&A 200, 85
Maeder A., Meynet G., 1989, A&A 210, 155
Matteucci F., François P., 1989, MNRAS 239, 885
Matteucci F., Franco J., François P., Treyer M.A., 1989, Rev. Mex. Astron. Astrofis. 18, 145
McClure R.D., 1989, in: Johnson H.R., Zuckerman B. (eds.) Evolution of Peculiar Red Giant Stars. Cambridge Univ. Press, Cambridge, p. 196
Paczynski B., 1970, Acta Astron. 20, 47
Paczynski B., 1971, Acta Astron. 21, 417
Paczynski B., 1975, ApJ 202, 558
Pagel B.E.J., Terlevich R.J., Melnick J., 1986, PASP 98, 1005
Panagia N., Gilmozzi R., Macchetto F., Adorf H.-M., Kirshner R.P., 1991, ApJ 380, L23
Payne-Gaposchkin C.M., 1971, Smithson. Contrib. Astrophys. 13, 1
Refsdal S., Weigert A., 1970, A&A 6, 426
Reid N., Tinney C., Mould J., 1990, ApJ 348, 98
Reimers D., 1975, in: Basheck B., et al. (eds.) Problems in Stellar Atmospheres and Envelopes. Springer, Berlin, p. 229
Reimers D., Koester D., 1988, A&A 202, 77
Reimers D., Koester D., 1989, A&A 218, 118
Renzini A., Voli M., 1981, A&A 94, 175 (RV)
Renzini A., Bernazzani M., Buonanno R., Corsi C.E., 1985, ApJ 294, L7
Richer H.B., 1981a, ApJ 243, 744
Richer H.B., 1981b, in: Iben I., Renzini A. (eds.) Physical Processes in Red Giants Stars. Reidel, Dordrecht, p. 153
Richer H.B., Olander N., Westerlund B.E., 1979, ApJ 230, 724
Rocca-Volmerange B., Schaeffer R., 1990, A&A 233, 427
Rood R.T., 1973, ApJ 184, 815
Russell S.C., Dopita M.A., 1990, ApJS 74, 93
Sackmann I.-J., 1980, ApJ 235, 554
Sackmann I.-J., Boothroyd B.S., 1991, ApJ 366, 529
Sackmann I.-J., Boothroyd B.S., Fowler W.A., 1990, ApJ 360, 727
Sagar R., Pandey K., 1989, A&A 79, 407
Scalo J.M., Miller G.E., 1979, ApJ 233, 596
Scalo J.M., Despain K.H., Ulrich R.K., 1975, ApJ 196, 805
Schönberner D., 1983, ApJ 272, 708
Schönberner D., 1991, Workshop on probable Post-AGB Stars, Leuven 10–11 October 1991 (in press)
Schwering P.B.W., 1988, Ph.D. Thesis, Leiden, p. 240
Searle L., Wilkinson A., Bagnuolo W.G., 1980, ApJ 239, 803
Smith V.V., Lambert D.L., 1986, ApJ 311, 843
Smith V.V., Lambert D.L., 1988, ApJ 333, 219
Spite F., Spite M., 1991a, in: Hayes R., Milne D. (eds.) The Magellanic Clouds, Reidel, Dordrecht, p. 243
Spite M., Spite F., 1991b, in: Hayes R., Milne D. (eds.) The Magellanic Clouds, Reidel, Dordrecht, p. 372
Steigman G., 1985, in: Arnett W., Truran J. (eds.) Nucleosynthesis: Challenges and New Developments, Chicago University Press, Chicago, p. 48
Steigman G., Gallagher J.S., Schramm D.N., 1989, Comm. Ap. 14, 97
Stothers R.B., 1991, ApJ 383, 820
Sugimoto D., 1971, Progr. Theor. Phys. 45, 761
Sweigart A.V., Greggio L., Renzini A., 1989, ApJS 69, 911
Sweigart A.V., Greggio L., Renzini A., 1990, ApJ 364, 527
Uus U., 1973, Nauch. Informatsii 26, 96
van den Hoek L.B., de Jong T., 1992, A&A (in preparation)
Weidemann V., Koester D., 1983, A&A 121, 77
Westerlund B.E., Olander N., Richer H.B., Crabtree D.R., 1978, A&AS 31, 61
Westerlund B.E., Azzopardi M., Breysacher J., Rebeirot E., 1991a, A&AS 91, 425
Westerlund B.E., Lequeux J., Azzopardi M., Reiberot E., 1991b, A&A 244, 367
Wheeler J.C., Sneden W., Truran J.W., 1989, ARA&A 27, 279
Wood P.R., 1981, in: Iben I., Renzini A. (eds.) Physical Processes in Red Giants. Kluwer, Dordrecht, p. 135
Wood P.R, 1987, in: Kwok S., Pottasch S.R. (eds.) Late Stages of Stellar Evolution. Kluwer, Dordrecht, p. 197
Wood P.R., 1990, in. Mennessier M.O., Omont A. (eds.) From Miras to Planetary Nebulae. Editions Frontieres, Gif-sur-Yvette, p. 67
Wood P.R., Zarro D.M., 1981, ApJ 247, 247
Wood P.R., Bessell M.S., Fox M.W., 1983, ApJ 272, 99
Wright F.W., Hodge P.W., 1971, AJ 76, 1003